Gastroenterology 2017;152:1462–1476

Farnesoid X Receptor Activation Promotes Hepatic Amino Acid Catabolism and Ammonium Clearance in Mice

Vittoria Massafra,[1] Alexandra Milona,[1] Harmjan R. Vos,[1] Rúben J. J. Ramos,[2] Johan Gerrits,[1,2] Ellen C. L. Willemsen,[1] José M. Ramos Pittol,[1] Noortje Ijssennagger,[1] Martin Houweling,[3] Hubertus C. M. T. Prinsen,[2] Nanda M. Verhoeven-Duif,[1,2] Boudewijn M. T. Burgering,[1] and Saskia W. C. van Mil[1]

[1]Center for Molecular Medicine, Universitair Medisch Centrum Utrecht, Utrecht, The Netherlands; [2]Department of Genetics, Universitair Medisch Centrum Utrecht, Utrecht, The Netherlands; and [3]Faculty of Veterinary Medicine, Utrecht University, Utrecht, The Netherlands

BACKGROUND & AIMS: The nuclear receptor subfamily 1 group H member 4 (NR1H4 or farnesoid X receptor [FXR]) regulates bile acid synthesis, transport, and catabolism. FXR also regulates postprandial lipid and glucose metabolism. We performed quantitative proteomic analyses of liver tissues from mice to evaluate these functions and investigate whether FXR regulates amino acid metabolism. **METHODS:** To study the role of FXR in mouse liver, we used mice with a disruption of *Nr1h4* (FXR-knockout mice) and compared them with floxed control mice. Mice were gavaged with the FXR agonist obeticholic acid or vehicle for 11 days. Proteome analyses, as well as targeted metabolomics and chromatin immunoprecipitation, were performed on the livers of these mice. Primary rat hepatocytes were used to validate the role of FXR in amino acid catabolism by gene expression and metabolomics studies. Finally, control mice and mice with liver-specific disruption of *Nr1h4* (liver FXR-knockout mice) were re-fed with a high-protein diet after 6 hours fasting and gavaged a $^{15}NH_4Cl$ tracer. Gene expression and the metabolome were studied in the livers and plasma from these mice. **RESULTS:** In livers of control mice and primary rat hepatocytes, activation of FXR with obeticholic acid increased expression of proteins that regulate amino acid degradation, ureagenesis, and glutamine synthesis. We found FXR to bind to regulatory sites of genes encoding these proteins in control livers. Liver tissues from FXR-knockout mice had reduced expression of urea cycle proteins, and accumulated precursors of ureagenesis, compared with control mice. In liver FXR-knockout mice on a high-protein diet, the plasma concentration of newly formed urea was significantly decreased compared with controls. In addition, liver FXR-knockout mice had reduced hepatic expression of enzymes that regulate ammonium detoxification compared with controls. In contrast, obeticholic acid increased expression of genes encoding enzymes involved in ureagenesis compared with vehicle in C57Bl/6 mice. **CONCLUSIONS:** In livers of mice, FXR regulates amino acid catabolism and detoxification of ammonium via ureagenesis and glutamine synthesis. Failure of the urea cycle and hyperammonemia are common in patients with acute and chronic liver diseases; compounds that activate FXR might promote ammonium clearance in these patients.

Keywords: Liver Proteome; INT-747; Cps1; Glutamine Synthetase.

Carbohydrates, proteins, and fats from the diet are digested in the gastrointestinal tract, where they are broken down into their basic units, sugars (monosaccharides, eg, glucose), amino acids, and free fatty acids, respectively. Via the portal venous circulation, these basic energy units reach the liver, where they are processed.[1] In the postprandial phase, glucose is used as energy source, condensed into glycogen, or converted into fatty acids or amino acids. Free fatty acids are either oxidized to generate energy or esterified with glycerol-3-phosphate to synthesize triacylglycerol and subsequently stored in the liver or distributed to other tissues via very low density lipoprotein (VLDL) incorporation. Amino acids are metabolized to provide energy or used to synthesize proteins, glucose, and/or other bioactive molecules.[2] Regulation of amino acid metabolism in the liver is crucial, because in times of dietary surplus, high concentrations of amino acids and ammonium reach the liver which may cause toxicity. Amino acids that are not used for protein synthesis are degraded to NH_4^+ and a carbon skeleton. Ammonium clearance is achieved by ureagenesis and glutamine synthesis in the liver.[3,4] Carbamoyl phosphate synthetase-1 (Cps1), catalyzes the committed step of ureagenesis and is mostly expressed in mitochondria of periportal hepatocytes, primarily exposed to intestinal protein catabolites. Glutamine synthesis relies on glutamine synthetase, Glul, expressed in cytosol of pericentral hepatocytes, where it ensures the clearance of ammonium and thereby controls tightly blood ammonium concentration.[5]

Next to their function as detergents facilitating dietary absorption of lipids and fat-soluble vitamins, bile acids (BAs) have an important function in regulation of nutrient

Abbreviations used in this paper: **BA, bile acid; ChIP, chromatin immunoprecipitation; Cps1, carbamoyl phosphate synthetase-1; FXR, Farnesoid X receptor; OCA, obeticholic acid; qPCR, quantitative polymerase chain reaction; TSS, transcription start site; Veh, vehicle; Wt, wild-type.**

Most current article

0016-5085
http://dx.doi.org/10.1053/j.gastro.2017.01.014

EDITOR'S NOTES

BACKGROUND AND CONTEXT

Bile acids regulate lipid and glucose metabolism via Farnesoid X Receptor (FXR) signaling in the enterohepatic circulation. The role of FXR of in the metabolism of the third category of nutrients, amino acids, was studied.

NEW FINDINGS

By using liver proteomic analyses combined with targeted metabolomics, the researchers show that FXR activation promotes amino acid catabolism and ammonium clearance through ureagenesis and glutamine synthesis in mice.

LIMITATIONS

This study focused on FXR function under normal physiological conditions, and does not provide direct evidence for therapeutic value of targeting FXR-mediated regulation of amino acid metabolism.

IMPACT

FXR agonists may ameliorate ammonium detoxification in patients with chronic liver disease.

metabolism.[6] By rapidly activating nuclear receptors and other cell signaling pathways upon their postprandial return to the liver, BAs not only induce feedback inhibition of BA synthesis, but also control lipid and glucose metabolism.[7]

Signaling of BAs in the postprandial phase is mediated by the farnesoid X receptor (FXR), which is mainly expressed in intestine, liver, and kidney. Intestinal FXR activation by BAs increases BA export into the portal circulation. In addition, FXR activation in the intestine increases Fgf15 synthesis and export into the portal system. Fgf15 through its membrane receptor Fgfr4 decreases hepatic BA biosynthesis, by affecting Cyp7a1 activity. Hepatic FXR activation increases BA efflux from hepatocytes through the regulation of BA transporter expression (eg, organic solute transporter (*OST*)-α/β, bile salt export pump (*BSEP*), and multidrug resistance protein type (*MDR*) 3).[8]

FXR modulates triacylglycerol clearance, by promoting lipoprotein lipase activity via induction of ApoC-II and controls fatty acid and cholesterol synthesis, via repression of Srebp1c. Moreover, FXR improves insulin sensitivity and glucose clearance via down-regulation of the gluconeogenic genes Pck1 and Fbp1.[9] Metabolic function of FXR as nutrient sensor encompasses also repression of autophagy during prolonged nutrient shortage.[10,11] Furthermore, FXR activation promotes liver regeneration and hepatocyte survival, inhibits hepatic inflammation, and enhances tumor suppressor genes.[12] FXR agonists were shown to be beneficial in clinical trials for nonalcoholic steatohepatitis and primary biliary cholangitis and may have therapeutic potential in gallstone disease, cirrhosis, liver cancer, and metabolic syndrome.[13]

In this study, we show that FXR not only regulates glucose and fatty acid metabolism, but also regulates the metabolism of the third class of basic energy units, that is, amino acids. We quantified liver proteome-wide changes occurring in vivo in response to obeticholic acid (OCA) or FXR ablation and confirmed the role of FXR in BA, lipid, and glucose metabolism. We show that FXR activation in vivo results in up-regulation of proteins involved in amino acid degradation, urea cycle, and glutamine synthesis, while FXR ablation associates with reduced expression of urea cycle proteins and accumulation of upstream substrates of urea cycle. FXR binds to regulatory sites of these genes and its activation increased urea production in primary hepatocytes. In vivo tracing studies of the conversion of isotopically labeled ammonium into urea also support a role for FXR in ureagenesis. Combining the data on FXR metabolic functions, we argue that FXR functions as a key regulator of deciding the postprandial fate of 3 three nutrient breakdown units: sugars, fats, and amino acids.

Materials and Methods

Animal Experiments

Homozygous FXR-floxed mice (C57BL/6 FXR fl/fl, kind gift from K. Schoonjans, Ecole Polytechnique Federale de Lausanne, Switzerland[14]) were crossed with Meox2-cre mice and Alb-Cre mice (Jackson Laboratory, Bar Harbor, ME) to generate whole-body FXR null mice ($FXR^{-/-}$), and liver-specific FXR-null mice (liver $FXR^{-/-}$) containing the same floxed allele for the ultimate comparison, respectively. FXR-floxed littermates without cre alleles were used as wild-type (Wt) controls. Genotyping of FXR-floxed mice was assessed as described previously.[14] FXR expression was assessed in liver, kidney, ileum, and adrenal glands of Meox2-cre mice ($FXR^{-/-}$) and Alb-cre mice ($livFXR^{-/-}$) (Supplementary Figure 1). Mice were fed a purified diet (AIN-93M, Research Diet, New Brunswick, NJ) ad libitum and housed in a temperature and light-controlled room. C57BL/6 male mice either WT or $FXR^{-/-}$ were gavaged with either OCA (10 mg/kg body weight, kindly provided by Luciano Adorini, Intercept Pharmaceuticals, San Diego, CA) or vehicle (Veh; 1% methyl cellulose) for 11 days. In the evening before sacrifice, mice received an extra gavage of OCA/Veh. Mice were fasted for 4 hours before sacrifice.

In an independent experiment, C57BL/6 male mice were gavaged with either OCA or Veh for 3 days. On day 3, mice were fasted for 6 hours. One group of mice were gavaged with $^{15}NH_4Cl$ dissolved in water (20 mg/kg body weight; Cambridge Isotope Laboratories, Tewksbury, MA) directly after fasting. Another group of mice were re-fed with a high-protein diet (ssniff EF R/M High Protein, E15209; ssniff Spezialdiäten GmbH, Soest, Germany) for 2 hours before they were gavaged the tracer. Mice were killed and livers and plasma were harvested 90 minutes after $^{15}NH_4Cl$ administration. Alb-cre mice ($livFXR^{-/-}$) and their Wt FXR fl/fl controls were subjected to the same treatment of re-feeding with high-protein diet and $^{15}NH_4Cl$ administration. All experiments were approved by the ethics committee of the University Medical Center Utrecht.

See Supplementary Methods for descriptions of the stable isotope labeling with amino acids in cell culture (SILAC)–based proteomics, primary hepatocyte culturing, urea, and amino acid mass spectrometry analyses.

Western Blotting

Liver tissue extracts were generated and protein concentration was assessed (BCA Assay Kit, Thermo Scientific,

Waltham, MA). Western blots were probed with antibodies against Cps1 (Origene, Rockville, MD), Ass1 (Abcam, Cambridge, UK), Glul (BD Biosciences, Franklin Lakes, NJ), Arg1 (Cell Signaling, Danvers, MA), Prodh (Abcam), and Hal (Abcam). α-Tubulin (Sigma, St Louis, MO), and α-actin (Abcam) antibodies were used as loading controls.

Chromatin Immunoprecipitation and Chromatin Immunoprecipitation Sequencing Analysis

Snap-frozen liver tissue was cross-linked with formaldehyde and processed for chromatin immunoprecipitation (ChIP) as described previously.[15] Primer sequences used for ChIP quantitative polymerase chain reaction (qPCR) are reported in Supplementary Table 1. IR1 motifs[16] were searched in peak regions proximal to target genes using the HOMER suite software. We analyzed ChIP-sequencing datasets generated in our laboratory (Gene Expression Omnibus, GSE73624[15]) and by others[17] to assess the binding profile of FXR in liver.

Gene Expression Analyses

RNA was isolated from primary hepatocytes using TRIzol reagent (Invitrogen, Carlsbad, CA). Complementary DNA was generated from 1 μg total RNA using SuperScript II Reverse Transcriptase (Invitrogen). Quantitative reverse transcription PCR analysis was performed using SYBR green PCR master mix (Roche, Basel, Switzerland) and analyzed on a MyIQ real-time PCR cycler (BioRad, Hercules, CA). Primer sequences are listed in Supplementary Table 2.

Statistics

Significance of pathway enrichment was determined by Ingenuity software, setting $P < .05$. Amino acid concentration in mouse liver tissue is expressed as mean ± SEM. Gene expression, amino acid, and urea concentration in primary hepatocytes are expressed as mean ± SD. Statistical significance was determined by Student t test using GraphPad software, version 6.02. Two-sided P values ($P < .05$) were considered significant.

Results

Liver Proteomic Analyses of Wild-Type and Farnesoid X Receptor Null Mice Treated With Obeticholic Acid

To determine the effects of FXR activation and ablation in the liver, we quantified protein expression changes in liver extracts from Wt and $FXR^{-/-}$ mice treated with Veh or OCA. Liver protein extracts (containing "light" lysine) were mixed 1:1 with a spike-in protein extract from $^{13}C_6$-lysine metabolically labeled mouse liver (containing "heavy" lysine) and analyzed by liquid chromatography tandem-mass spectrometry (Figure 1*A*). Spike-in efficiency, indicating the quality of the heavy signal as internal standard, was assessed as frequency of proteins in the Veh-treated mice ranked based on their $\log_2$ heavy to light normalized ratio (Figure 1*B*). Most proteins had a heavy to light ratio close to 1, indicating a substantial equality in protein composition of the liver from the mice in the experiment and the "heavy" liver tissue, thereby supporting the suitability of the heavy labeled liver as internal standard for the light samples.

Our proteomic analysis identified 4514 proteins, of which 3070 were identified with 2 or more unique peptides, were not reverse hits, decoy hits, or standard contaminants; 2354 proteins were quantified with a $\log_2$ light to heavy normalized ratio. FXR activation by OCA resulted in up-regulation of 5% of proteins and down-regulation of 10% of proteins quantified, whereas FXR ablation resulted in a more profound impact on the proteome (23% proteins were up-regulated, 34% were down-regulated, Figure 1*C*).

There were 2244 proteins quantified in each experimental condition (Wt Veh, Wt OCA, $FXR^{-/-}$ Veh, $FXR^{-/-}$ OCA; n = 1), enabling comparative analyses of protein expression (Figure 1*D*). Hierarchical clustering of quantified proteins based on their light to heavy normalized ratios revealed 2 general clustered regions that include proteins with decreased or increased expression in $FXR^{-/-}$ compared with Wt mice (Figure 1*E*). Within each of these clusters, subsets of proteins could be identified, which were up-regulated or down-regulated upon OCA only in the Wt, only in the $FXR^{-/-}$ or in both genotypes. Three hundred and seventy proteins were regulated in an FXR-dependent manner after treatment with OCA: 122 proteins were up-regulated in the Wt, but not in the $FXR^{-/-}$ mice, whereas 248 proteins were down-regulated by OCA in the Wt, but not in the $FXR^{-/-}$ mice. Genetic FXR ablation had a stronger impact on liver proteome: 454 proteins were up-regulated, and 739 down-regulated in both Veh and OCA-treated mice (Figure 1*F*).

Regulation of Bile Acid Metabolism by Farnesoid X Receptor Is Supported by Liver Proteomic Analyses

To validate the quality of our proteome dataset, we analyzed protein changes in BA metabolism pathways. Protein expression of the BA transporter Bsep (Abcb11) increased in Wt mice treated with OCA and decreased in $FXR^{-/-}$ compared with Wt mice (Figure 2*A* and *B*), in line with FXR-dependent increase in efflux of BAs from the liver to the canalicular lumen.[8,18] Oppositely, the BA synthesis enzyme Cyp8b1 decreased in Wt mice treated with OCA and increased in $FXR^{-/-}$ mice (Figure 2*A* and *B*), in line with previous reports.[19] In Figure 2*C* (and Supplementary Table 3), a schematic overview is given of protein expression changes induced by FXR activation/ablation with regard to BA metabolism. Similar to Cyp8b1, expression of Cyp7a1 was up-regulated by FXR ablation, however, because Cyp7a1 could not be quantified in Wt mice (possibly because the expression was very low upon OCA treatment), a ratio between OCA- and Veh-treated mice could not be determined. Expression of the rate-limiting enzyme of the taurine metabolism Csad decreased 1.6-fold upon FXR activation and increased 9.3-fold upon FXR ablation, supporting the role of FXR in regulating taurine availability and BA conjugation, in line with a previous report.[20]

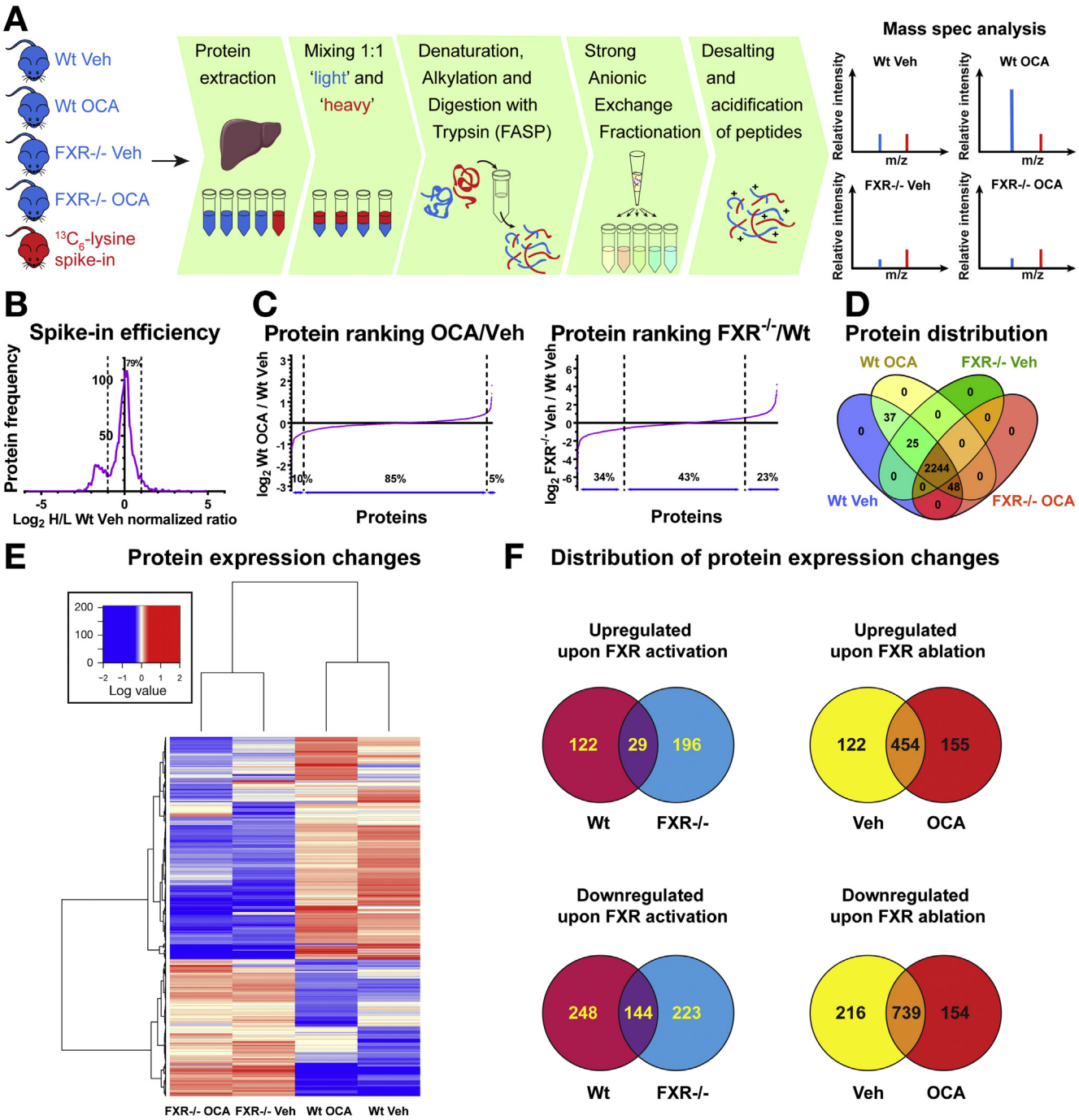

Figure 1. Proteomic analysis in liver tissue derived from Wt and FXR$^{-/-}$ mice treated with or without OCA. (*A*) Experimental outline to determine the proteome of mouse liver extracts by liquid chromatography tandem-mass spectrometry. (*B*) Frequency plot of proteins identified in Veh-treated Wt mice based on their total $\log_2$ heavy to light normalized ratio. The plot is representative of a Wt untreated condition to show the basal efficiency of the heavy spike-in added to the light samples. Percentage of proteins with a $\log_2$ heavy to light normalized ratio included in interval $(-1, +1)$ is shown. (*C*) Protein ranking based on changes of the $\log_2$ light to heavy normalized ratio induced by FXR activation (*left panel*) and ablation (*right panel*). Percentages of proteins, of which expression was decreased (≤ -1.3-fold), unchanged, or increased (≥ 1.3-fold), are indicated. (*D*) *Venn diagram* summarizing the distribution of quantified proteins in each of the 4 experimental groups (Wt Veh, Wt OCA, FXR$^{-/-}$ Veh, FXR$^{-/-}$ OCA). (*E*) Comparative heat-map analysis of the effect of FXR activation and ablation on mouse liver proteome. Proteins were clustered from the top to the bottom based on similar expression profile in the 4 experimental groups (Wt Veh, Wt OCA, FXR$^{-/-}$ Veh, FXR$^{-/-}$ OCA). (*F*) *Venn diagram* showing the number of proteins regulated by OCA in Wt mice and in FXR$^{-/-}$ mice (*left panel*) and upon FXR ablation in Veh and OCA-treated mice (*right panel*). Only fold changes ≥ 1.3 were considered.

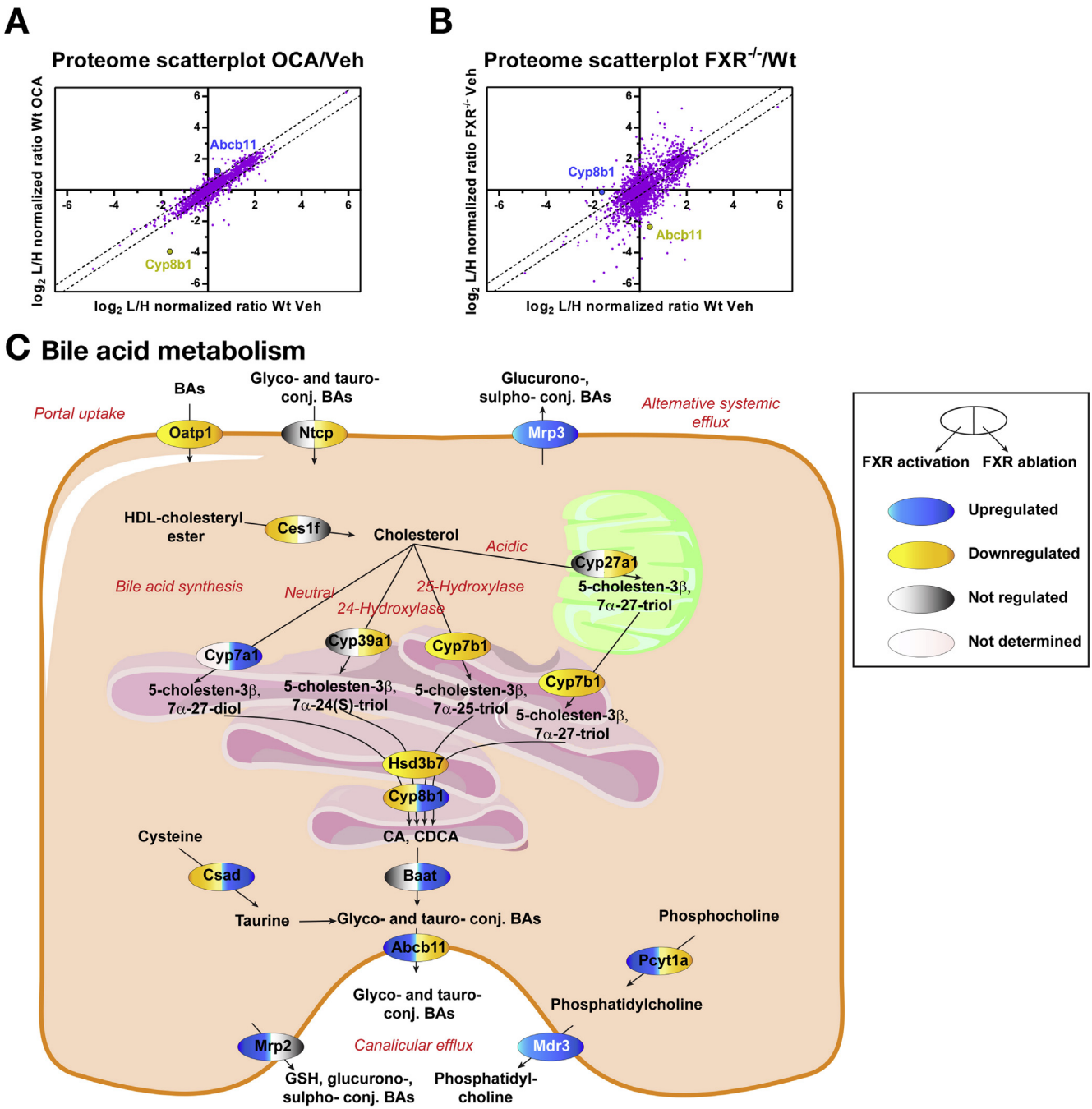

Figure 2. Proteome-wide changes in BA metabolism. (*A, B*) Protein *scatterplots* depicting proteome-wide changes on FXR activation (*A*) and ablation (*B*) in liver. Abcb11 (Bsep) and Cyp8b1 are *highlighted* as representative proteins related to BA metabolism known to be up- or down-regulated by FXR activation, respectively. (*C*) Schematic representation of protein expression changes (≥1.4 fold) of relevance for BA metabolism (*B*). Up-regulated (*blue*), down-regulated (*yellow*), or unchanged (*gray*) proteins on OCA treatment (*left half box*) or FXR ablation (*right half box*). Nonquantified changes are indicated in *white*.

Protein expression of Slc10a1 (Ntcp), which guides the portal uptake of conjugated BAs, was severely reduced in $FXR^{-/-}$, which does not concur with the equal mRNA levels of Ntcp reported in Wt and $FXR^{-/-}$ mice,[21] but is concurrent with data showing that Ntcp protein expression is reduced in conditions of hepatic BA retention (like in cholestasis or in $FXR^{-/-}$ mice).[22] Finally, expression of Abcc3 (Mrp3), which promotes systemic efflux of conjugated BAs, was up-regulated upon OCA treatment (2.0-fold), consistent with FXR induction of basolateral transporters promoting systemic secretion of BAs.[23]

In summary, our proteomic analyses recapitulate the role of FXR in down-regulation of BA synthesis, regulation of

BA conjugation, and up-regulation of BA efflux into the canalicular lumen and in the systemic circulation.

A Novel Role for Farnesoid X Receptor in Regulation of the Third Class of Basic Energy Units: Amino Acids

Having validated our dataset, we next used our proteomic data to gain insights into novel biological functions of FXR. We performed pathway and ontology analyses on all differentially expressed proteins (Figure 3*A* and Supplementary Figure 2). Similar metabolic pathways were found to be regulated by FXR activation and ablation. As expected, FXR/retinoid X receptor activation and activation of other nuclear receptors functionally related to FXR were among the most significantly changed pathways upon FXR activation/ablation (*black bars*). Likewise, FXR activation/ablation impacts on BA, cholesterol, and steroid metabolism (*yellow bars*) and on metabolism of fatty acids, glucose, and glutathione metabolism (*gray, blue*, and *purple bars*, respectively), as has been shown previously.[7,24,25] Strikingly, FXR activation and ablation significantly changed protein expression concerning amino acid metabolism, including urea cycle, citrulline, tryptophan, tyrosine, alanine, glycine, histidine, phenylalanine, methionine, glutamine, glutamate, and proline metabolism (*green bars*). This pathway enrichment analysis suggests that FXR regulation of nutrient metabolism applies to dietary basic units of lipids, and carbohydrates, but also extends to catabolic products of the third main energy source: proteins.

In Figure 3*B*, we schematically depicted the changes in protein expression in amino acid catabolism pathways upon FXR activation and FXR ablation (Supplementary Table 4). FXR activation increased the expression of multiple enzymes in the pathway of conversion of histidine to glutamate (Hal, Uroc1, Amdhd1, Ftcd) and of proline to glutamate (Prodh). FXR activation also increased expression of enzymes relevant for tryptophan (Tdo2, Kynu), methionine (Mat1a, Ahcy, Cth), phenylalanine (Pah), and 5-hydroxylysine (Agphd1) degradation. On the other hand, FXR ablation resulted in down-regulation of most of the proteins mentioned related to amino acid degradation. Together, these results suggest that FXR mediates the induction of hepatic amino acid catabolism.

In postprandial state, clearance of hepatic ammonium generated from intestinal catabolism and hepatic amino acid catabolism requires the conversion into urea or glutamine.[3,4] Expression of enzymes of urea cycle Ass1, Asl, and Arg1 were up-regulated by FXR activation and down-regulated by FXR ablation. Cps1 and Nags—key enzymes of urea cycle—and Gls2 and Glud1, which provide mitochondrial glutamate and ammonium to urea cycle, respectively, were unchanged or down-regulated upon FXR activation, but were strongly reduced in expression in $FXR^{-/-}$ mice.

We also observed FXR-dependent regulation of Glul, which was up-regulated by OCA (1.5-fold) and down-regulated upon FXR ablation (2.2-fold). Glul is important for alternative disposal of ammonium via conversion of glutamate to glutamine, especially in pericentral hepatocytes,[3] suggesting a role of FXR in ammonium detoxification via glutamine synthesis as well.

By immunoblot analyses, we confirmed that expression of Cps1, Ass1 and Arg1, Glul, Hal and Prodh were indeed reduced upon FXR ablation and increased or unchanged upon FXR activation, although the effect of FXR ablation was more pronounced (Figure 3*C*), concurrent with the proteomic data. The changes in protein expression induced by OCA are rather small or undetected, but the sensitivity of the immunoblot assay does not allow picking small changes in protein expression. In addition, the small changes in protein expression may be due to the dynamic regulation of protein expression, that is, we may be too early or too late after OCA stimulation to appreciate the largest fold difference compared with unstimulated mice. To validate the role of FXR in amino acid catabolism and ureagenesis, we have analyzed FXR transcriptional regulation of these enzymes and amino acid and urea production in primary hepatocytes and liver-specific FXR knockouts in subsequent experiments.

Farnesoid X Receptor Binds to Gene Regulatory Sites of Enzymes in the Urea Cycle and Amino Acid Catabolism Pathways

To investigate whether FXR regulates the transcription of genes involved in amino acid metabolism, we analyzed genome-wide FXR binding profiles in mouse liver in a ChIP-sequencing dataset generated in our laboratory,[15] and by Thomas et al.[17] FXR peaks were identified within 10 kb from the transcription start site (TSS) of the genes *Glul*, *Ass1*, *Asl*, *Hal*, and *Prodh*, and within 45 kb from the TSS of *Cps1* (Figure 4*A*, and Supplementary Table 1). We searched for IR1 sites, the preferential binding motif for FXR,[16] in the selected peaks (Supplementary Table 1) and to validate FXR binding to these sites, we performed ChIP-qPCR using primers designed around the identified IR1 motifs. We confirmed FXR binding to 2 peaks upstream of the TSS and a peak in an intronic region of *Cps1*, and to a peak in the promoter of *Hal* and *Glul*, in an intronic region of *Asl* and *Prodh* and upstream of the TSS of *Ass1* (Figure 4*B*). *Globin* and *Fabp6* (FXR target gene in intestine, not in liver) promoters were used as negative control regions, whereas *Slc51b* (Ostβ), *Nr0b2* (Shp), and *Abcb11* promoters were used as positive controls for FXR binding. These data provide evidence for a role of FXR as direct transcriptional regulator of enzymes involved in urea cycle, glutamine synthesis, and histidine and proline catabolism.

Farnesoid X Receptor Ablation Results in Accumulation of Urea Cycle Precursors in the Liver

Next, we investigated whether FXR-mediated regulation of amino acid metabolism induced changes in amino acid concentrations in liver extracts (Figure 5 and Supplementary Table 5). Precursors for the urea cycle—glutamate, glutamine, and aspartate—were increased in

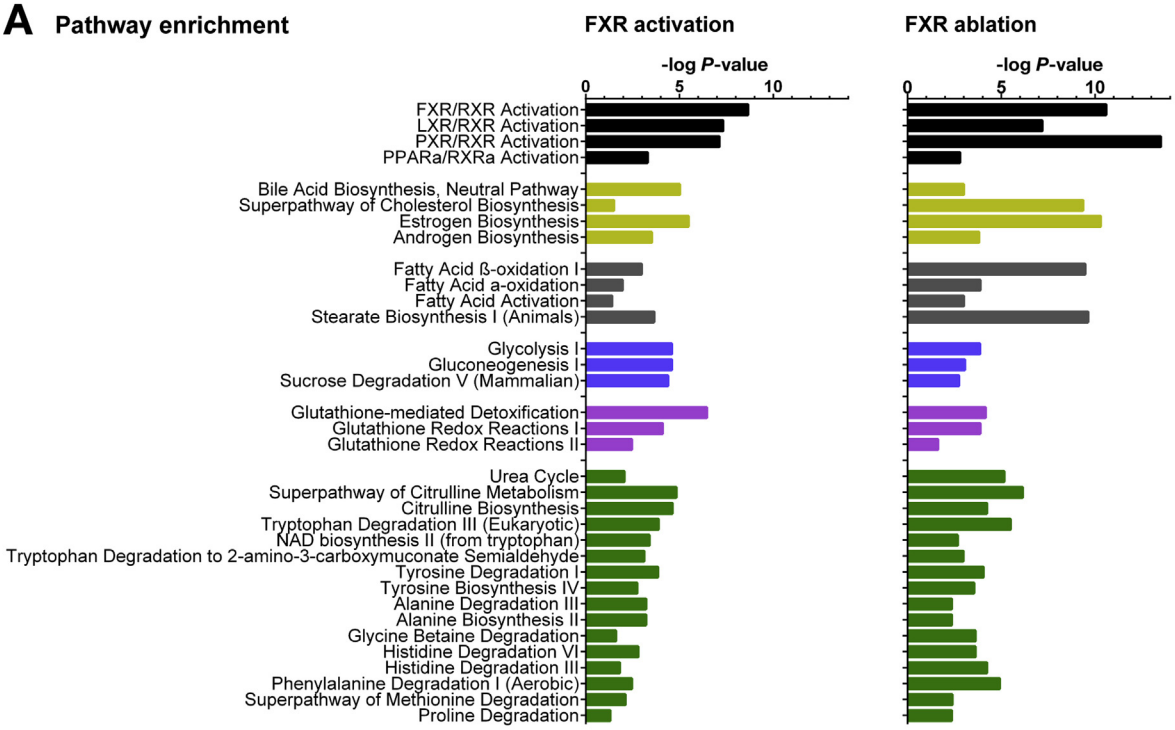
A Pathway enrichment
FXR activation
FXR ablation
-log P-value
0
5
10
FXR/RXR Activation
LXR/RXR Activation
PXR/RXR Activation
PPARa/RXRa Activation
Bile Acid Biosynthesis, Neutral Pathway
Superpathway of Cholesterol Biosynthesis
Estrogen Biosynthesis
Androgen Biosynthesis
Fatty Acid ß-oxidation I
Fatty Acid a-oxidation
Fatty Acid Activation
Stearate Biosynthesis I (Animals)
Glycolysis I
Gluconeogenesis I
Sucrose Degradation V (Mammalian)
Glutathione-mediated Detoxification
Glutathione Redox Reactions I
Glutathione Redox Reactions II
Urea Cycle
Superpathway of Citrulline Metabolism
Citrulline Biosynthesis
Tryptophan Degradation III (Eukaryotic)
NAD biosynthesis II (from tryptophan)
Tryptophan Degradation to 2-amino-3-carboxymuconate Semialdehyde
Tyrosine Degradation I
Tyrosine Biosynthesis IV
Alanine Degradation III
Alanine Biosynthesis II
Glycine Betaine Degradation
Histidine Degradation VI
Histidine Degradation III
Phenylalanine Degradation I (Aerobic)
Superpathway of Methionine Degradation
Proline Degradation

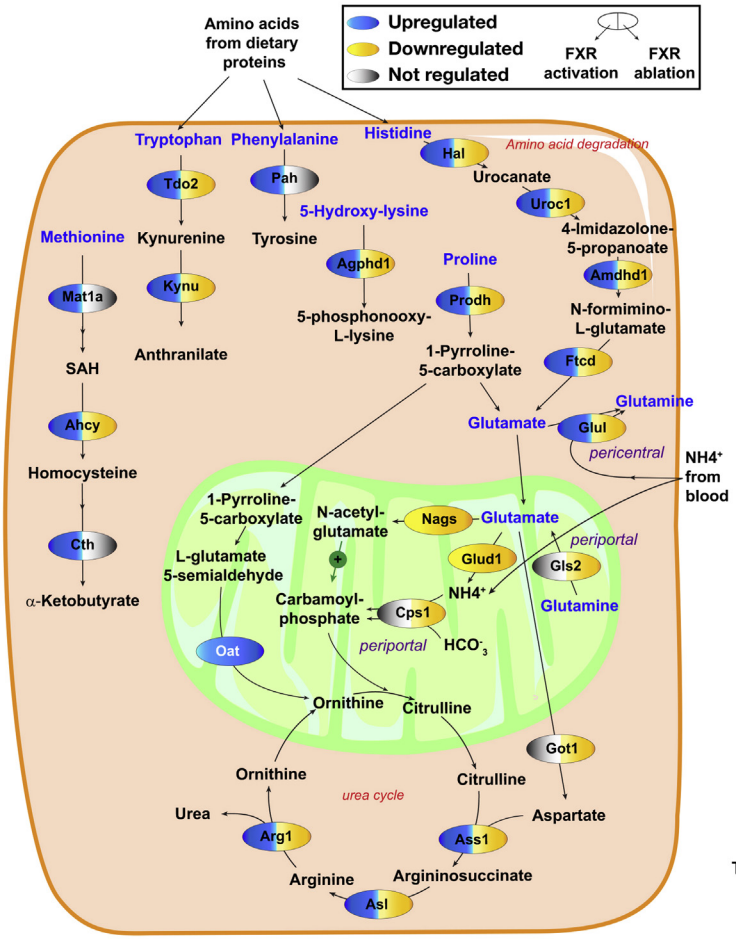
B Amino acid metabolism
Upregulated
Downregulated
Not regulated
FXR activation
FXR ablation
Amino acids from dietary proteins
Tryptophan
Phenylalanine
Histidine
Amino acid degradation
Hal
Urocanate
Tdo2
Pah
Uroc1
4-Imidazolone-5-propanoate
Amdhd1
N-formimino-L-glutamate
Ftcd
Methionine
Kynurenine
Tyrosine
5-Hydroxy-lysine
Agphd1
5-phosphonooxy-L-lysine
Proline
Prodh
1-Pyrroline-5-carboxylate
Mat1a
SAH
Kynu
Anthranilate
Ahcy
Homocysteine
Cth
α-Ketobutyrate
Glutamine
Glutamate
Glul
pericentral
NH4+ from blood
1-Pyrroline-5-carboxylate
N-acetyl-glutamate
Nags
Glutamate
periportal
Glud1
Gls2
L-glutamate 5-semialdehyde
NH4+
Glutamine
Carbamoyl-phosphate
Cps1
HCO3-
periportal
Oat
Ornithine
Citrulline
Got1
Ornithine
Citrulline
urea cycle
Urea
Aspartate
Arg1
Ass1
Arginine
Argininosuccinate
Asl

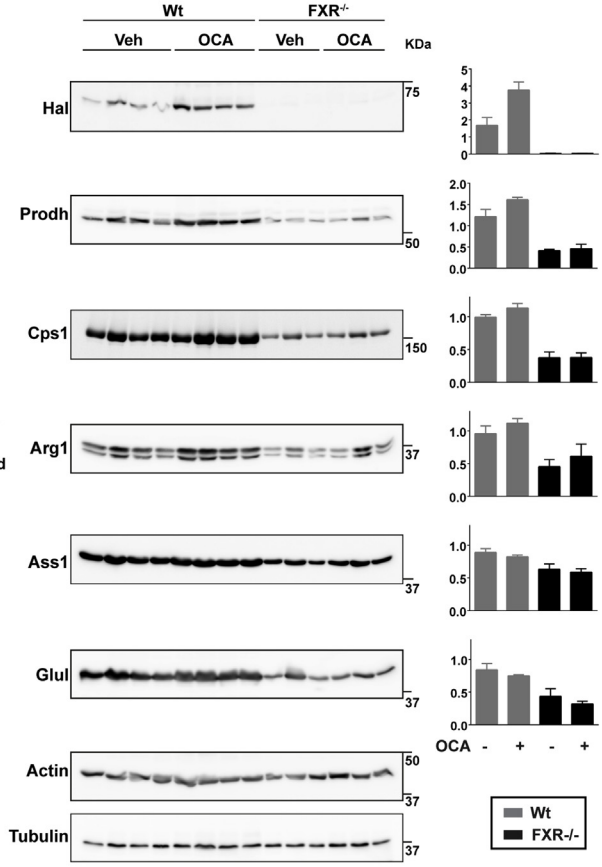
C
Wt
FXR-/-
Veh
OCA
Veh
OCA
KDa
Hal
75
Prodh
50
Cps1
150
Arg1
37
Ass1
37
Glul
37
Actin
50
37
Tubulin
37
OCA - + - +
Wt
FXR-/-

mouse livers of $FXR^{-/-}$ compared with Wt mice, whereas urea cycle intermediates citrulline and ornithine were decreased, indicative of a stagnation of the urea cycle in the liver (Figure 5*A* and *B*). Histidine increased in $FXR^{-/-}$ compared with Wt mice, in line with reduced expression of histidine degrading enzymes, such as Hal (Figure 5*B*). No significant changes in amino acid concentrations were detected upon OCA treatment in Wt mice. FXR depletion in mice is expected to result in hyperammonemia and a decrease in plasma urea concentration. Actually, $FXR^{-/-}$ mice, but not liver $FXR^{-/-}$ mice, showed an increase in plasma urea concentrations compared with Wt mice (Figure 5*C*). These results have to be interpreted considering that plasma urea concentration is the final result of intestinal protein breakdown, liver urea production, degradation of urea by ureases of gastrointestinal bacteria, and renal excretion of urea into urine,[26] and may therefore not reflect amino acid catabolism and urea production by the liver. Therefore, in the next series of experiments, we have relied on primary hepatocyte sandwich cultures and short-term OCA treatments as well as in vivo tracing experiments in liver-specific knockout mice to ascertain whether FXR directly regulates amino acid catabolism and urea production.

Farnesoid X Receptor Activation Increases Gene Expression of Glutamine Synthetase and Urea Cycle-Related Genes and Enhances Urea Production in Primary Rat Hepatocytes

To investigate whether FXR directly regulates transcription of genes involved in amino acid metabolism, we stimulated sandwich cultures of primary rat hepatocytes with OCA for 0, 1, 4, or 17 hours. Efficient activation of FXR by OCA treatment was evaluated by increased mRNA expression of the FXR target gene *Shp* and decreased mRNA expression of *Cyp7a1*, which are known to be repressed by Shp (Figure 6*A*). We confirmed that *Glul*, *Ass1*, *Asl*, and *Prodh* are increased upon FXR activation by OCA, albeit with different expression kinetics (Figure 6*A*). Expression of Cps1 and Hal increased slightly, but not significantly (Figure 6*A*). FXR activation determined a less-robust regulation of genes involved in amino acid metabolism compared with Shp and Cyp7a1, classically linked to bile acid metabolism. Nevertheless, the OCA-dependent increase in expression of urea cycle genes concurred with a significant increase in the amount of urea produced in the medium in 1 hour, after 20 hours of OCA stimulation (Figure 6*B*). Taken together, these data indicate that FXR directly increases expression of genes involved in glutamine synthesis, urea cycle and proline catabolism, and causes a concurrent increase in urea production.

Farnesoid X Receptor Activation Promotes Glutamine Synthesis and Urea Production on Ammonium Excess

In order to validate whether FXR promotes expression of genes involved in glutamine synthesis and urea cycle to ensure detoxification of ammonium in excess after feeding, we exposed primary rat hepatocytes to FXR agonists for 6 hours, and in the last hour before harvesting, we exposed the cells to excess of NH_4Cl, ornithine, and glutamine (Figure 6*C*). *Shp* mRNA increased upon treatment with OCA or with the synthetic FXR agonist GW4064, as expected (Figure 6*D*). Expression of *Cps1* increased 2-fold after OCA or GW4064 treatment when excess ammonium was present (Figure 6*D*), suggesting that FXR-mediated induction *Cps1* is dependent on the ammonium concentration, because we did not observe Cps1 induction in the absence of ammonium (Figure 6*A*). Expression of *Glul* was also induced by OCA and GW4064, indicating that the investigated effects can be ascribed to FXR-mediated mechanisms rather than FXR-independent BA functions. In agreement with the induced expression of genes involved in the urea cycle, urea production increased after exposure to OCA or GW4064 (Figure 6*E*).

To further characterize the effects of OCA on amino acid metabolism, we measured amino acid concentrations in medium of primary hepatocytes incubated for 16 hours with OCA or dimethyl sulfoxide and in the last hour before harvesting with NH_4Cl, glutamine, and ornithine. The concentration of glutamate decreased upon OCA treatment (Figure 6*E* and Supplementary Table 6), in line with FXR promoting the catabolism of key amino acids shuttling ammonium groups into the urea cycle. Despite the increase in Glul expression, glutamine concentration did not increase upon OCA treatment, likely as a result of decreased substrate, glutamate. Also the concentration of histidine and proline decreased upon OCA treatment, in line with the FXR-mediated induction of the protein expression of Hal and Prodh, responsible for the degradation of histidine and proline. Together, our results indicate that FXR activation ensures the nitrogen homeostasis in hepatocytes by facilitating detoxification of the ammonium groups from excess dietary amino acids by increasing ureagenesis and glutamine synthesis.

Figure 3. FXR activation regulates amino acid metabolism. (*A*) Canonical pathway analysis (using Ingenuity Pathway analysis software) of protein expression changes with fold-change ≥1.3 upon FXR activation and ablation. Pathways are clustered with similar colors based on their overall function. (*B*) Schematic representation of protein expression changes (≥1.4-fold) related to amino acid metabolism. Up-regulated (*blue*), down-regulated (*yellow*), or unchanged (*gray*) proteins upon OCA treatment (*left half box*) or FXR ablation (*right half box*). (*C*) Western blot analysis of proteins involved in amino acid catabolism (Hal, Prodh), urea cycle (Cps1, Ass1, Arg1), and glutamine synthesis (Glul) in liver extracts harvested from Wt or $FXR^{-/-}$ mice treated with either Veh or OCA. Actin and tubulin were used as loading controls. Protein extracts from 4 Wt mice and from 3 $FXR^{-/-}$ mice were included in the analysis. Quantification is shown relative to tubulin and actin.

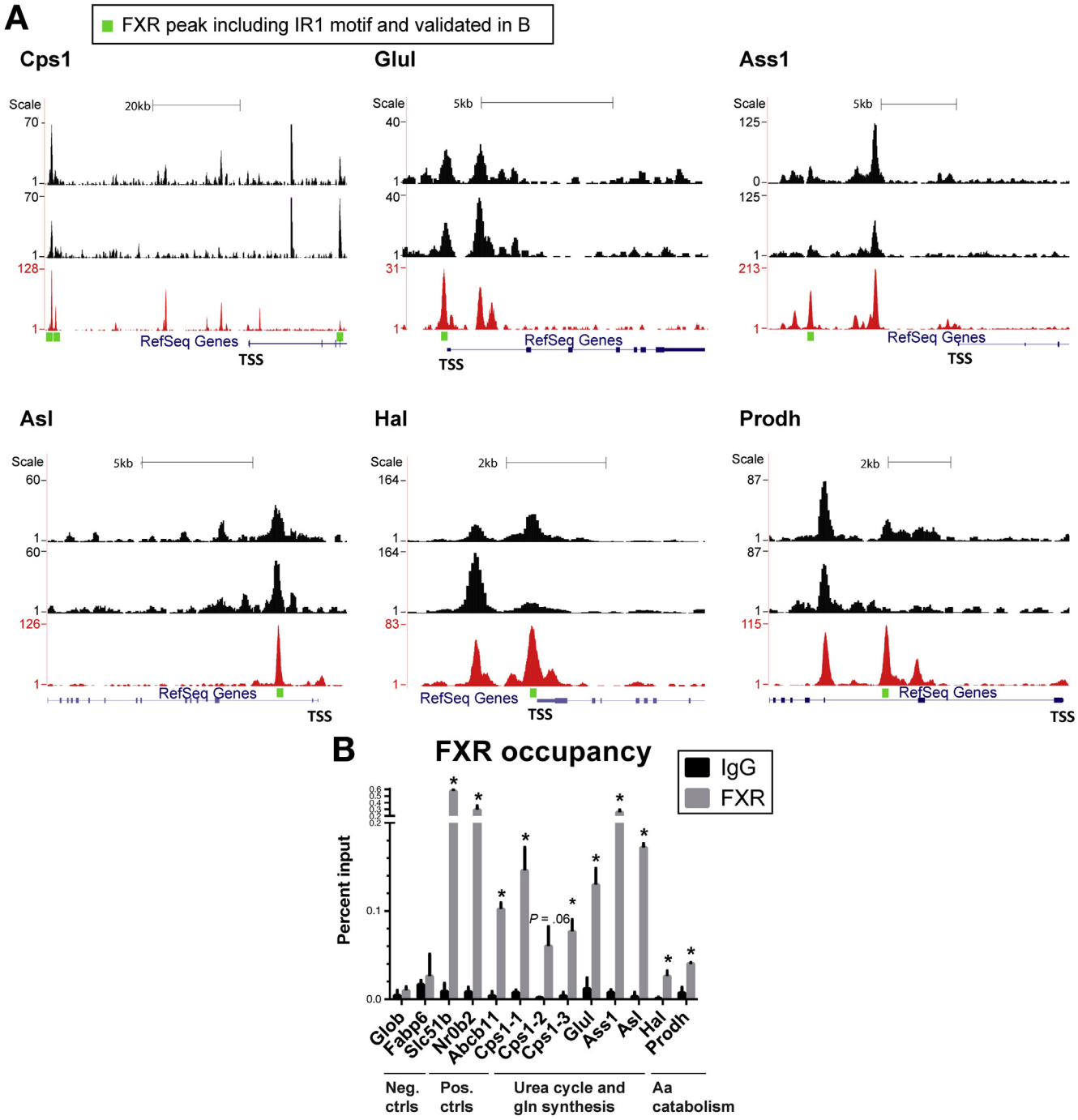

Figure 4. FXR binds to gene regulatory sites of genes encoding enzymes involved in amino acid catabolism, urea cycle, and glutamine synthesis. (*A*) FXR ChIP sequencing (seq) tracks from liver of 2 Wt mice are depicted in *black*.[15] The *red track* refers to a ChIP-seq experiment in mouse liver.[17] FXR enrichment at genomic regions proximal to *Cps1*, *Glul*, *Ass1*, *Asl*, *Hal*, and *Prodh* is shown. *Green boxes* indicate the peaks, including the IR1 motif in which FXR binding was validated by ChIP-qPCR. (*B*) Validation of candidate peaks by ChIP-qPCR in liver extracts from Wt mice. *Globin* and *Fabp6* regions were used as negative controls and *Slc51b* (Ostβ), *Nr0b2* (Shp), and *Abcb11* (Bsep) were used as positive controls for FXR occupancy in the liver. Data are shown as mean ± SD, n = 2. *$P < .05$ by Student *t*-test.

Farnesoid X Receptor Regulates Ureagenesis in vivo

Finally, we set out to measure newly formed urea from a gavaged $^{15}NH_4Cl$ tracer in mice. Mice were fasted for 6 hours and half of the group was re-fed with high-protein diet for 2 hours (Figure 7*A*). Based on the experiment performed by Youdkhoff et al,[27] we measured plasma ^{15}N-urea 90 minutes after $^{15}NH_4Cl$ administration. Under these conditions, ^{15}N-urea in re-fed mice increased on OCA treatment, although it did not reach statistical significance ($P = .09$)

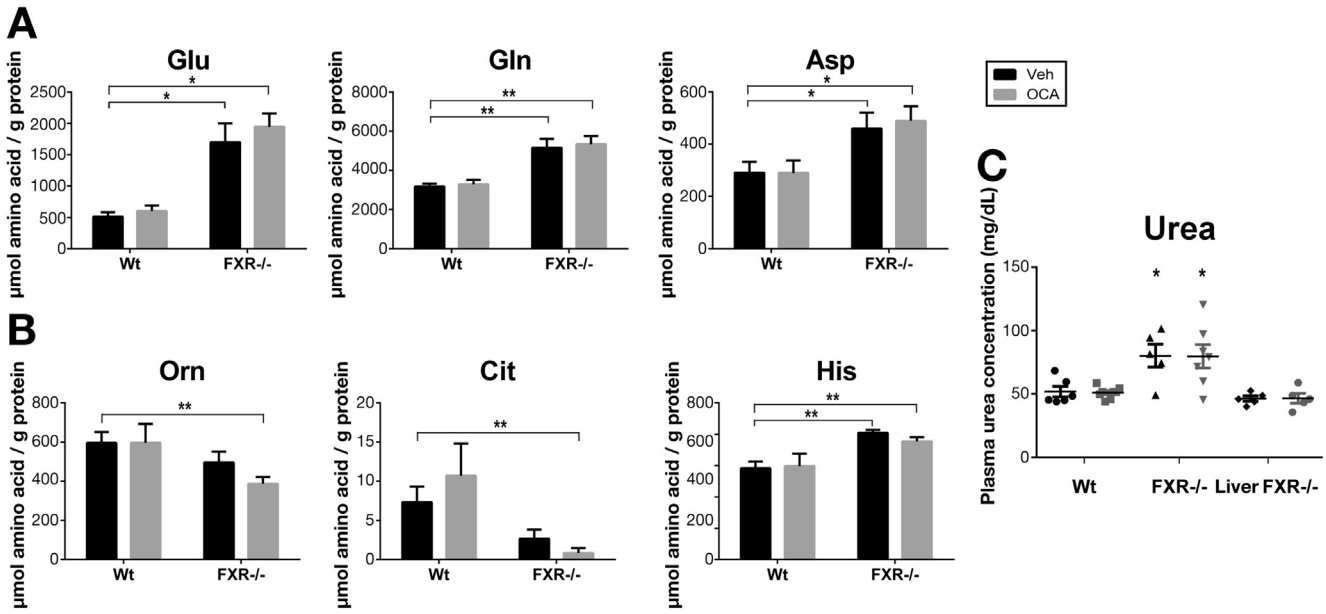

Figure 5. FXR ablation causes accumulation of urea cycle precursors in the liver. (*A*, *B*) Determination of amino acid concentrations in liver extracts harvested from Wt or $FXR^{-/-}$ mice treated with either Veh or OCA for 11 days (n = 5–7/group). Amino acid concentrations are normalized to protein concentration in the liver extract. Data are shown as mean ± SEM, $^{*}P < .05$ by 2-way analysis of variance test. (*C*) Plasma urea concentrations, as measured using QuantiChrom TM Urea Assay kit, in Wt and total $FXR^{-/-}$, and liver-specific $FXR^{-/-}$ mice treated with either Veh or OCA (n = 5–8/group). Data are shown as mean ± SEM. $^{*}P < .05$ by Mann-Whitney test compared with the respective treatment in Wt mice.

(Figure 7*B*). This was not seen in fasted mice. The concentration of ^{14}N-urea did not change upon treatment with OCA in plasma from either fasted or re-fed mice, presumably as a consequence of the compensatory increase in renal excretion. Concomitantly, OCA treatment resulted in significant increases in *Bsep*, *Glul*, and *Gls2,* and almost significant increase in *Ass1* expression (Figure 7*C*). Administration of $^{15}NH_4Cl$ to liver-specific $FXR^{-/-}$ and their Wt FXR fl/fl controls (Figure 7*D*) after fasting and re-feeding a high-protein diet significantly reduced ^{15}N-urea plasma concentration in liver-specific $FXR^{-/-}$ mice compared with the Wt FXR fl/fl controls (Figure 7*E*), while the concentration of unlabeled ^{14}N-urea was unchanged (data not shown). Concurrent with an impaired formation of newly generated urea, liver-specific $FXR^{-/-}$ mice display higher plasma concentrations of the precursor amino acids for ureagenesis glutamine and glutamate than their respective controls. Finally, liver-specific FXR deletion reduced the expression of FXR target *Bsep* and of the genes *Glul*, *Gls2*, *Ass1*, *Nags*, and *Prodh* (Figure 7*F*). In conclusion, FXR regulates amino acid catabolism in the liver in vivo, by acting as a transcriptional regulator of enzymes involved in urea cycle and glutamine synthesis.

Discussion

Nitrogen homeostasis after feeding involves the degradation of amino acids taken up from the diet that are not required for net protein or neurotransmitter synthesis.[28] These surplus amino acids are degraded to ammonium (NH_4^+) and a carbon skeleton. The carbon skeleton can be used for the production of glucose or fatty acids. Nitrogen derived from the catabolism of these surplus amino acids cannot be physiologically stored and depends on ureagenesis and glutamine synthesis for appropriate disposal or temporary storage.[3] A major determinant of the rate of ureagenesis is substrate availability. In addition, glucagon, insulin, and glucocorticoids have been shown to modulate the activity of enzymes in the urea cycle.[5] Noteworthy, transcriptional control of urea cycle genes has also been reported. Hepatocyte nuclear factor (*Hnf*) 4α increases expression of ornithine carbamoyl transferase, *Otc.* Peroxisome proliferator-activated receptor (*Ppar*)$-\alpha$ and CCAAT/enhancer binding protein (*C/Ebp*)$-\alpha$ have been shown to oppositely regulate expression of the urea cycle genes *Cps1, Otc, Ass1, Asl, and Arg1.*[29] However, the complex interplay of transcription factors in coordinating ureagenesis is far from being understood completely.

FXR is a nutrient-sensing nuclear receptor activated by BAs in the intestine and in the liver; it is an important regulator of glucose and fat metabolism.[30] We have combined an in vivo SILAC–based method with filter-aided sample preparation–strong anion exchange (FASP-SAX) to determine the proteome-wide expression changes in mouse liver in response to FXR activation by OCA. To our knowledge, this is the first time that such an approach was used to validate and extend established functions of FXR, as well as to investigate unexplored FXR functions. We showed that FXR activation down-regulates BA synthesis, modulates BA conjugation, and up-regulates BA efflux into the canalicular lumen and in the systemic circulation, in line with what it is

reported in literature.[7] Overall, FXR ablation had a stronger effect on the liver proteome than OCA treatment, as shown in Figure 1. FXR ablation resulted in suppression of Cyp7b1, Cyp27a1, Ntcp, and Oatp1 expression and up-regulation of Abcc3, which are likely to be consequences of increased BA hepatic retention in $FXR^{-/-}$ mice leading to a reduction in BA synthesis and BA uptake and an increase in BA efflux to compensate for the BA retention in the liver. We concluded

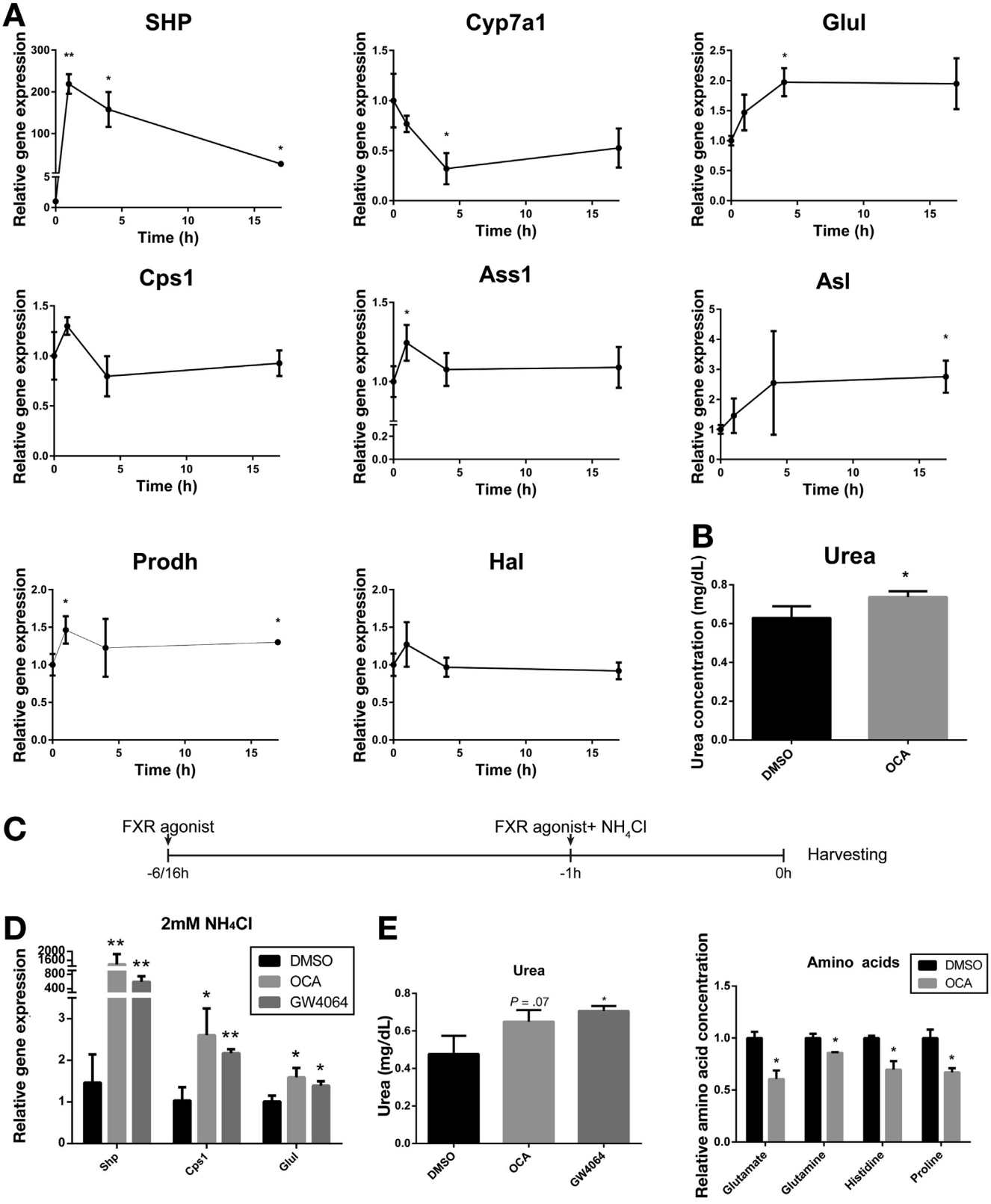

that the proteomic dataset proved to be a valid tool to investigate additional FXR functions.

In agreement with a previous report,[31] our quantitative proteome analyses support a role for FXR in ureagenesis. However, our data implicate that the role of FXR in amino acid metabolism extends to regulation of general dietary amino acid breakdown and nitrogen disposal via glutamine synthesis and ureagenesis. Indeed, protein expression of enzymes degrading histidine (Hal, Uroc1, Amdhd1, Ftcd) was induced upon OCA treatment in Wt mice, and suppressed in $FXR^{-/-}$ mice. The concentrations of histidine in liver extracts of $FXR^{-/-}$ mice were increased, concurrent with decreased expression of enzymes involved in its catabolism. OCA treatment in primary hepatocytes decreased the histidine concentration in the medium, and because FXR induced the expression of Hal and binds to an IR1 motif in the proximity of the TSS of Hal, we conclude that this is due to direct FXR-transcriptional regulation of Hal. Similarly, FXR binding to the promoter of Prodh was confirmed and proline concentration was decreased, while Prodh expression was increased upon OCA treatment in primary hepatocytes, indicating that also proline catabolism is directly regulated by FXR.

Furthermore, OCA induced the enzymes in the urea cycle Ass1, Asl, and Arg1, whereas FXR ablation caused suppression of urea cycle enzymes (Nags, Cps1, Ass1, Asl, Arg1). In contrast to Renga et al,[31] we do not find evidence for a direct role of FXR in the regulation of Nags (Supplementary Figure 3), which converts glutamate to N-acetyl glutamate, the latter being an essential allosteric activator of Cps1. We currently do not understand this discrepancy, but it may depend on the culture conditions of the primary hepatocytes. Lastly, FXR activation by OCA induced the expression of Glul, which converts glutamate into glutamine in pericentral hepatocytes, an alternative way to dispose of excess nitrogen.[4] Our quantitative proteomic data are in agreement with mass spectrometry identification of proteins detected by 2D-DIGE by Gardmo et al,[32] listing that FXR activation similarly leads to induced expression of Glud1, Got2, Ass1, Arg1, Cps1, and Oat.

Genetic FXR ablation promotes hepatic steatosis, hyperlipidemia, impaired glucose tolerance, and hepatic BA accumulation.[14,21,33] Here we show that $FXR^{-/-}$ mice accumulate glutamine, glutamate, and aspartate in the liver (Figure 5), which represent the key amino acids for shuttling ammonium groups into the urea cycle. If liver ureagenesis would reflect plasma urea concentrations, it is expected that urea production would be decreased in $FXR^{-/-}$ mice. In fasted state, $FXR^{-/-}$ mice, but not liver $FXR^{-/-}$ mice, actually accumulate urea in the plasma (Figure 5*G*). The amount of urea in plasma is controlled also by renal excretion, which requires glomerular filtration, urea concentration in the urine by urea transporter UT-B (Slc14a1) and urea reabsorption in the blood by UT-A (Slc14a2).[26,34,35] Intriguingly, FXR is expressed in kidney and our analysis of microarray datasets available online[36] revealed that UT-B is significantly up-regulated (3.5-fold) in kidney cells treated with GW4064, while UT-A is unchanged. From these data, it could be speculated that renal FXR promotes urea excretion and works in concert with hepatic FXR to ensure the clearance of excess ammonium. This might explain the difference in plasma urea concentrations in total and liver $FXR^{-/-}$ mice. Importantly, liver-specific FXR deletion reduced formation of ^{15}N-urea from $^{15}NH_4Cl$ tracer in mice re-fed with a high-protein diet, indicating that an ammonium excess may be required for triggering FXR–dependent regulation of ureagenesis. Interorgan compensation complicates the detection of oscillations in total plasma urea in response to drugs, however, OCA-treatment induced an almost significant increase in plasma ^{15}N-urea, newly formed from the gavaged $^{15}NH_4Cl$ tracer. Indeed, FXR activation promoted urea production and increased the expression of *Glul*, *Ass1*, *Asl*, and *Cps1* expression also in primary hepatocytes, especially in conditions of ammonium excess (Figure 6).

We further show that FXR binds to the IR1 motifs in proximity of the transcription start sites of *Cps1*, *Glul*, *Ass1*, and *Asl,* indicating that FXR directly regulates transcription of urea cycle and glutamine synthesis genes. OCA increased while liver-specific FXR deletion decreased hepatic gene expression of the Ass1, Glul, and Gls2, implicated in ammonium detoxification, also in mice re-fed with a high-protein diet, further substantiating the relevance of this regulation in vivo.

mTORC1 is a protein complex that functions as a sensor for essential amino acids and controls protein synthesis by activation of the translation initiation complex.[28,37,38] The activity of the mTORC1 complex is regulated by insulin, growth factors, and amino acids. We hypothesize that FXR

Figure 6. FXR activation promotes glutamine synthesis and urea production in sandwich cultures of primary rat hepatocytes. (*A*) Relative gene expression of *Shp*, *Cyp7a1*, *Glul*, *Cps1*, *Ass1*, *Asl*, *Prodh*, and *Hal* was assessed by qRT-PCR. Expression at each time point is normalized to its respective dimethyl sulfoxide (DMSO) control. Gene expression data were normalized to 36b4 (Rplp0). Significant changes compared with t = 0 are indicated with an *asterisk*. (*B*) Urea concentrations in medium of sandwich cultures of primary hepatocytes treated with DMSO or OCA for 20 hours. One hour before harvesting, the medium was changed to 10 mM HEPES in Hank's balanced salt solution (HBSS) to measure urea release. (*C*) Experimental outline of treated primary rat hepatocytes. Primary hepatocytes were incubated with DMSO, 1 μM OCA, or GW4064 for 6 hours (for gene expression and urea) or 16 hours (for amino acid measurements). One hour before harvesting, the medium was changed to 2 mM NH_4Cl, 0.4 mM glutamine, 0.6 mM ornithine, and 10 mM HEPES in HBSS. (*D*) Relative gene expression of *Shp, Glul,* and *Cps1* was investigated by qRT-PCR (*E*) Urea (*left panel*) and amino acid (*right panel*) concentrations in medium of primary hepatocytes treated with FXR agonists. All data are shown as mean ± SD (n = 3), significant changes ($P < .05$ by a Student *t* test) compared with DMSO are indicated with an *asterisk*.

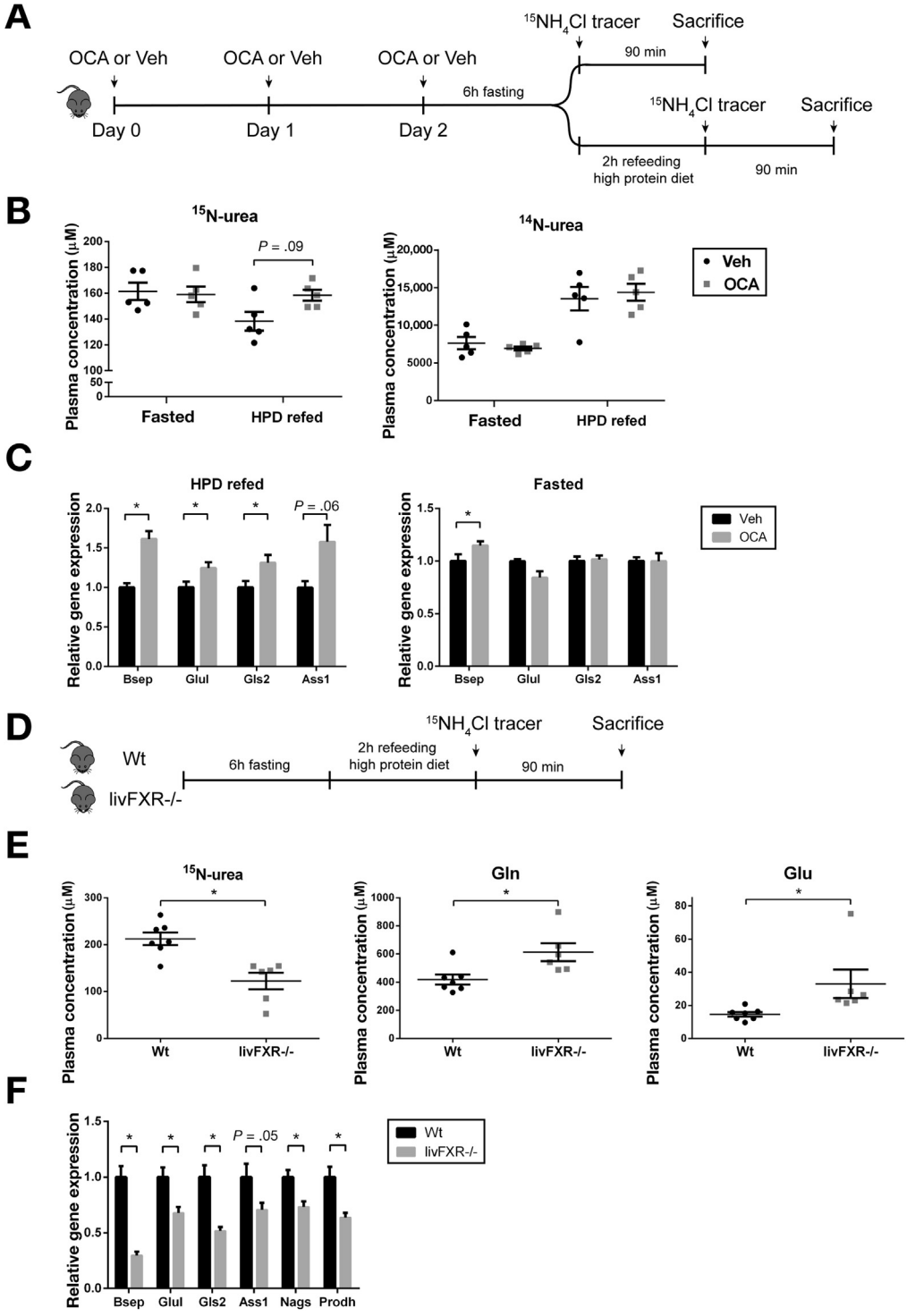

Figure 7. FXR regulates ureagenesis in vivo. (*A*) Experimental outline to assess FXR regulation of ammonium detoxification in Wt mice fasted for 6 hours with or without re-feeding with a high-protein diet. (*B*) ^{14}N- and ^{15}N- plasma urea concentrations determined by mass spectrometry analysis in Wt mice fasted or re-fed treated with either Veh or OCA for 3 days. (*C*) Relative gene expression of *Bsep, Glul, Gls2,* and *Ass1*. (*D*) Experimental outline to assess FXR regulation of ammonium detoxification in liver-specific FXR$^{-/-}$ and their respective Wt controls (FXR fl/fl) fasted for 6 hours and re-fed with a high-protein diet. (*E*) ^{15}N plasma urea, glutamine, and glutamate concentrations. (*F*) Relative gene expression of *Bsep, Glul, Gls2*, *Ass1*, *Nags*, and *Prodh*. Gene expression data were normalized to cyclophilin. Data are shown as mean ± SEM (n = 5–7/group). *$P < .05$ by Mann-Whitney test.

may counterbalance mTORC1 activity by inducing amino acid catabolism if proteins are in surplus.

In conclusion, our study identifies FXR as transcriptional regulator of amino acid catabolism and detoxification of ammonium via ureagenesis and glutamine synthesis in the liver. Because urea cycle failure and hyperammonemia are common complications of acute and chronic liver diseases,[39,40] FXR activation could represent a new therapeutic strategy to promote ammonium clearance in liver disease patients.

Supplementary Material

Note: To access the supplementary material accompanying this article, visit the online version of *Gastroenterology* at www.gastrojournal.org, and at http://dx.doi.org/10.1053/j.gastro.2017.01.014.

References

1. Kohlmeier M. Nutrient Metabolism. Food Science and Technology, International Series. London: Academic Press, 2003.
2. Rui L. Energy metabolism in the liver. Compr Physiol 2014;4:177–197.
3. Adeva MM, Souto G, Blanco N, et al. Ammonium metabolism in humans. Metabolism 2012;61:1495–1511.
4. Rodes J. Textbook of Hepatology: from Basic Science to Clinical Practice. Malden, MA: Blackwell, 2007.
5. Morris SM Jr. Regulation of enzymes of the urea cycle and arginine metabolism. Annu Rev Nutr 2002;22:87–105.
6. Zhou H, Hylemon PB. Bile acids are nutrient signaling hormones. Steroids 2014;86:62–68.
7. Lefebvre P, Cariou B, Lien F, et al. Role of bile acids and bile acid receptors in metabolic regulation. Physiol Rev 2009;89:147–191.
8. Mazuy C, Helleboid A, Staels B, et al. Nuclear bile acid signaling through the farnesoid X receptor. Cell Mol Life Sci 2015;72:1631–1650.
9. Gadaleta RM, Cariello M, Sabba C, et al. Tissue-specific actions of FXR in metabolism and cancer. Biochim Biophys Acta 2015;1851:30–39.
10. Lee JM, Wagner M, Xiao R, et al. Nutrient-sensing nuclear receptors coordinate autophagy. Nature 2014;516:112–115.
11. **Seok S, Fu T**, Choi SE, et al. Transcriptional regulation of autophagy by an FXR-CREB axis. Nature 2014;516:108–111.
12. Huang X, Zhao W, Huang W. FXR and liver carcinogenesis. Acta Pharmacol Sin 2015;36:37–43.
13. Neuschwander-Tetri BA. Farnesoid x receptor agonists: what they are and how they might be used in treating liver disease. Curr Gastroenterol Rep 2012;14:55–62.
14. **Milona A, Owen BM**, van Mil S, et al. The normal mechanisms of pregnancy-induced liver growth are not maintained in mice lacking the bile acid sensor Fxr. Am J Physiol Gastrointest Liver Physiol 2010;298:G151–G158.
15. Ijssennagger N, Janssen AW, Milona A, et al. Gene expression profiling in human precision cut liver slices upon treatment with the FXR agonist obeticholic acid. J Hepatol 2016;64:1158–1166.
16. Chong HK, Infante AM, Seo YK, et al. Genome-wide interrogation of hepatic FXR reveals an asymmetric IR-1 motif and synergy with LRH-1. Nucleic Acids Res 2010;38:6007–6017.
17. Thomas AM, Hart SN, Kong B, et al. Genome-wide tissue-specific farnesoid X receptor binding in mouse liver and intestine. Hepatology 2010;51:1410–1419.
18. Suchy FJ, Ananthanarayanan M. Bile salt excretory pump: biology and pathobiology. J Pediatr Gastroenterol Nutr 2006;43(Suppl 1):S10–S16.
19. Kong B, Wang L, Chiang JY, et al. Mechanism of tissue-specific farnesoid X receptor in suppressing the expression of genes in bile-acid synthesis in mice. Hepatology 2012;56:1034–1043.
20. **Kerr TA, Matsumoto Y**, Matsumoto H, et al. Cysteine sulfinic acid decarboxylase regulation: a role for farnesoid X receptor and small heterodimer partner in murine hepatic taurine metabolism. Hepatol Res 2014;44:E218–E228.
21. **Sinal CJ, Tohkin M**, Miyata M, et al. Targeted disruption of the nuclear receptor FXR/BAR impairs bile acid and lipid homeostasis. Cell 2000;102:731–744.
22. Geier A, Wagner M, Dietrich CG, et al. Principles of hepatic organic anion transporter regulation during cholestasis, inflammation and liver regeneration. Biochim Biophys Acta 2007;1773:283–308.
23. Modica S, Gadaleta RM, Moschetta A. Deciphering the nuclear bile acid receptor FXR paradigm. Nucl Recept Signal 2010;8:e005.
24. Jin J, Sun X, Zhao Z, et al. Activation of the farnesoid X receptor attenuates triptolide-induced liver toxicity. Phytomedicine 2015;22:894–901.
25. Livero FA, Stolf AM, Dreifuss AA, et al. The FXR agonist 6ECDCA reduces hepatic steatosis and oxidative stress induced by ethanol and low-protein diet in mice. Chem Biol Interact 2014;217:19–27.
26. Weiner ID, Mitch WE, Sands JM. Urea and ammonia metabolism and the control of renal nitrogen excretion. Clin J Am Soc Nephrol 2015;10:1444–1458.
27. Yudkoff M, Daikhin Y, Ye X, et al. In vivo measurement of ureagenesis with stable isotopes. J Inherit Metab Dis 1998;21(Suppl 1):21–29.
28. Bender DA. The metabolism of “surplus” amino acids. Br J Nutr 2012;108(Suppl 2):S113–S121.
29. Desvergne B, Michalik L, Wahli W. Transcriptional regulation of metabolism. Physiol Rev 2006;86:465–514.
30. Teodoro JS, Rolo AP, Palmeira CM. Hepatic FXR: key regulator of whole-body energy metabolism. Trends Endocrinol Metab 2011;22:458–466.
31. Renga B, Mencarelli A, Cipriani S, et al. The nuclear receptor FXR regulates hepatic transport and metabolism of glutamine and glutamate. Biochim Biophys Acta 2011;1812:1522–1531.
32. Gardmo C, Tamburro A, Modica S, et al. Proteomics for the discovery of nuclear bile acid receptor FXR targets. Biochim Biophys Acta 2011;1812:836–841.
33. Ma K, Saha PK, Chan L, et al. Farnesoid X receptor is essential for normal glucose homeostasis. J Clin Invest 2006;116:1102–1109.
34. Yang B. Urea Transporters. New York: Springer, 2014.
35. Yang B, Bankir L, Gillespie A, et al. Urea-selective concentrating defect in transgenic mice lacking urea transporter UT-B. J Biol Chem 2002;277:10633–10637.
36. Gui T, Gai Z. Genome-wide profiling to analyze the effects of FXR activation on mouse renal proximal tubular cells. Genom Data 2015;6:31–32.
37. Chandel NS. Navigating Metabolism. Cold Spring Harbor, NY: Cold Spring Harbor Laboratory Press, 2015:128.
38. **Zoncu R, Efeyan A**, Sabatini DM. mTOR: from growth signal integration to cancer, diabetes and ageing. Nat Rev Mol Cell Biol 2011;12:21–35.

39. Blei AT, Cordoba J. Practice Parameters Committee of the American College of Gastroenterology. Hepatic encephalopathy. Am J Gastroenterol 2001;96:1968–1976.
40. Nicaise C, Prozzi D, Viaene E, et al. Control of acute, chronic, and constitutive hyperammonemia by wild-type and genetically engineered *Lactobacillus plantarum* in rodents. Hepatology 2008;48:1184–1192.

Author names in bold designate shared co-first authorship.

Received March 29, 2016. Accepted January 17, 2017.

Reprint requests
Address requests for reprints to: Saskia W. C. van Mil, PhD, Center for Molecular Medicine, UMC Utrecht, HP 3.217, PO Box 85060, 3508 AB Utrecht, The Netherlands. e-mail: S.W.C.vanMil@umcutrecht.nl; fax: +31 88 7568101.

Conflicts of interest
The authors disclose no conflicts.

Funding
Saskia W. C. van Mil is supported by the Netherlands Organization for Scientific Research (NWO) Project VIDI (917.11.365), FP7 Marie Curie Actions IAPP (FXR-IBD, 611979), the Utrecht University Support Grant, Wilhelmina Children's Hospital Research Fund. Harmjan R. Vos is supported by Proteins At Work (NWO).

Supplementary Methods

Reagents

DL-Glutamic acid (2,4,4-D3, 98%), and urea (15N2, 98%) were purchased from Cambridge Isotope Laboratories (Cambridge, MA). Urea was purchased from Sigma-Aldrich (Zwijndrecht, the Netherlands). Glutamic acid and glutamine were purchased from VWR (Amsterdam, the Netherlands). Ultra-performance liquid chromatography–grade acetonitrile and methanol were purchased from Biosolve (Valkenswaard, the Netherlands).

Mass Spectrometry Sample Preparation for Proteomics

Liver protein extracts were generated by homogenizing 50 mg liver tissue in phosphate-buffered saline and subsequent lysis in lysis buffer (1% NP40, 150 mM NaCl, 1 mM dithiothreitol, 50 mM Tris [pH 8.0], Roche Proteinase inhibitors). Next, 100 μg protein extract from Wt or FXR$^{-/-}$ mice ("light") were mixed 1:1 with a spike-in protein extract generated from $^{13}C_6$-lysine metabolically labeled mouse liver ("heavy") (Silantes, Munich, Germany), using the same homogenization protocol. Proteins were denatured in urea, alkylated with iodoacetamide (Sigma, St Louis, MO) and digested with 1 μg trypsin (Promega, Fitchburg, WI) using a filtered aided sample purification protocol.[1] After trypsinization, peptides were fractionated based on their pH using strong anionic exchange chromatography and finally desalted and acidified on a C-18 cartridge (3M, St Paul, MN). C-18 stagetips were activated with methanol, washed with buffer containing 0.5% formic acid in 80% acetonitrile (buffer B), and then with 0.5% formic acid (buffer A). After loading of the digested sample, stagetips were washed with buffer A and peptides were eluted with buffer B, dried in a SpeedVac, and dissolved in buffer A.

Stable Isotope Labeling With Amino Acids in Cell Culture–Based Proteomics and Data Analysis

Peptides were separated on-a 30 cm column (75-μm ID fused silica capillary with emitter tip, New Objective, Woburn, MA) packed with 3-μm aquapur gold C-18 material (Dr Maisch, Ammerbuch-Entringen, Germany) using a 4-hour gradient (buffer A to buffer B), and delivered by an easy nanoflow high-performance liquid chromatography (nHPLC) (Thermo Scientific, Waltham, MA). Peptides were electrosprayed directly into a LTQ-Verlos-Orbitrap (Thermo Scientific) and analyzed in data-dependent mode with the resolution of the full scan set at 60,000, after which the top 10 peaks were selected for collision-induced dissociation (CID) fragmentation in the Iontrap with a target setting of 5000 ions.

Raw files were analyzed with Maxquant software, version 1.5.1.0.[2] For identification, the mouse Uniprot 2012 database was searched with peptide and protein false discovery rates set to 1%. The stable isotope labeling with amino acids in cell culture (SILAC) quantification algorithm was used in combination with the "match between runs" tool (option set at 2 minutes), the IBAQ and the LFQ algorithms.[3,4] Proteins identified with 2 or more unique peptides were filtered for reverse hits, decoy hits, and standard contaminants using Perseus software, version 1.3.0.4.[5] Normalized ratios were used to quantify protein expression and further processed for comparative analysis of differential expression among the experimental conditions. Heatmap visualization of expression profile of all quantified proteins was generated using R Studio (0.99.879). The mass spectrometry proteomics data have been deposited to the ProteomeXchange Consortium via the PRIDE[6] partner repository with the dataset identifier PXD005427. Analyzed data are presented in the Supplementary Data File. Pathway and ontology analyses were performed by Ingenuity Pathway analysis (Qiagen, Venlo, The Netherlands) and David Gene Ontology tools.

Primary Hepatocyte Culture

Hepatocytes were isolated from male Wistar rats (160–180 g) based on a 2-step collagenase perfusion method.[7] Hepatocytes were counted using Countess (Invitrogen, Waltham, MA) and cell viability was determined using Trypan blue. Freshly isolated hepatocytes with a viability of at least 85% were plated on collagen-coated plates. Sandwich cultures of primary hepatocytes were prepared by covering attached hepatocytes with collagen.[8] After 48 hours, hepatocytes were incubated with 1 μM OCA, 1 μM GW4064, or dimethyl sulfoxide. To evaluate gene expression changes in presence of ammonium excess and to determine urea production, we incubated hepatocytes with Hank's balance salt solution containing 10 mM HEPES, 2 mM NH_4Cl, 0.4 mM L-glutamine, and 0.6 mM ornithine for 1 hour at 37°C in a humidified atmosphere with 5% CO_2. Urea concentration in the medium was measured using QuantiChrom Urea Assay kit (Bioassay Systems, Hayward, CA).

Analysis of Amino Acids by Liquid Chromatography-Tandem Mass Spectrometry

Frozen liver tissue was homogenized in phosphate-buffered saline using a Tissue Lyzer II (Qiagen). Amino acid concentrations in liver extracts were determined by ultra-performance liquid chromatography tandem mass spectrometry as described previously.[9] Apart from adapting the range of the calibrators and quality-control samples, no further adaptations were needed for sample preparation or analysis of the amino acids. Data were normalized to protein concentration. Similarly, amino acid concentrations were determined in medium harvested from primary hepatocytes.

Analysis of Labeled Urea, Glutamine, and Glutamate by Liquid Chromatography–High Resolution Mass Spectrometry

A volume of 40 μL plasma was mixed with 20 μL of an internal standard solution in methanol consisting of labeled amino acids and urea (see Table 1 for the concentrations).

Table 1. Concentration of Standards

Internal standard	IS solution concentration, μM	Standard	Concentration range, μM
$^{2}H_3$-glutamate	500	Glutamate	0.5–250
$^{15}N_2$-urea	2257	Urea	45–24000

IS, internal standard.

After adding 500 μL methanol and vortexing for 30 seconds, the sample was centrifuged 13,000 rpm for 5 minutes. The supernatant was pipetted in an Eppendorf tube and evaporated under a gentle flow of nitrogen at 40°C. The extract was dissolved in 200 μL of a mixture of eluent A/B (10/90% v/v) and 10 μL was analyzed on the ultra-high-performance liquid chromatography system. For calibration, to 40 μL pool plasma a volume of 20 μL standards diluted in methanol was added (see Table 1 for the concentration range), and the same procedure was followed. Some of the amino acids were calculated on different labeled internal standards, see Table 1. The ^{15}N-isotopes were calculated on the ^{14}N-isotope calibration curves.

Liquid Chromatography/High-Resolution Mass Spectrometry Conditions

For the chromatographic separation, a ZIC-pHILIC column, 150 × 4.6 mm, 5-μm and guard column 20 × 2.1 mm; obtained from HiChrom (Reading, UK) was used at a working temperature of 40°C. A Thermo Scientific Ultimate 3000 UHPLC system controlled by Dionex chromatography MS Link 2.14 software (Thermo Fisher Scientific) combined with a Q-Exactive HF mass spectrometer from Thermo Fisher Scientific (Bremen, Germany) was employed as the liquid chromatography/high-resolution mass spectrometry platform in this study. Samples were kept at 15°C during the analyses.

The mobile phase used was 20 mM ammonium carbonate buffer (pH 9.2) as eluent A and pure acetonitril as eluent B. The elution gradient was programed at a flow of 0.3 mL/min as decreasing the percentage of B from 90% to 20% in 30 minutes, followed by washing the column at 5% of B for 5 minutes and finally re-equilibrating the column at 90% of B for 10 minutes. The ESI interface was operated in a positive polarity mode at a spray voltage of 4.0 kV. The temperature of the ion transfer capillary was 320°C and sheath and auxiliary gas was 40 and 8 arbitrary units, respectively. The full scan range was 55 to 400 m/z with settings of automatic gain control target at $1e^6$ and resolution of 120,000, respectively. The S-lens radio-frequency level was set at 50. The data were recorded using Xcalibur 4.0 software (Thermo Fisher Scientific). The quantification was done in Tracefinder 4.0 (Thermo Fisher Scientific).

References

1. Wisniewski JR, Zougman A, Mann M. Combination of FASP and StageTip-based fractionation allows in-depth analysis of the hippocampal membrane proteome. J Proteome Res 2009;8:5674–5678.
2. Cox J, Mann M. MaxQuant enables high peptide identification rates, individualized p.p.b.-range mass accuracies and proteome-wide protein quantification. Nat Biotechnol 2008;26:1367–1372.
3. **Luber CA, Cox J**, Lauterbach H, et al. Quantitative proteomics reveals subset-specific viral recognition in dendritic cells. Immunity 2010;32:279–289.
4. Schwanhausser B, Busse D, Li N, et al. Global quantification of mammalian gene expression control. Nature 2011;473:337–342.
5. Cox J, Mann M. 1D and 2D annotation enrichment: a statistical method integrating quantitative proteomics with complementary high-throughput data. BMC Bioinformatics 2012;13(Suppl 16):S12.
6. Vizcaino JA, Csordas A, del-Toro N, et al. 2016 update of the PRIDE database and its related tools. Nucleic Acids Res 2016;44:D447–D456.
7. Seglen PO. Preparation of isolated rat liver cells. Methods Cell Biol 1976;13:29–83.
8. Chatterjee S, Bijsmans IT, van Mil SW, et al. Toxicity and intracellular accumulation of bile acids in sandwich-cultured rat hepatocytes: role of glycine conjugates. Toxicol In Vitro 2014;28:218–230.
9. Prinsen HC, Schiebergen-Bronkhorst BG, Roeleveld MW, et al. Rapid quantification of underivatized amino acids in plasma by hydrophilic interaction liquid chromatography (HILIC) coupled with tandem mass-spectrometry. J Inherit Metab Dis 2016;39:651–660.

Author names in bold designate shared co-first authorship.

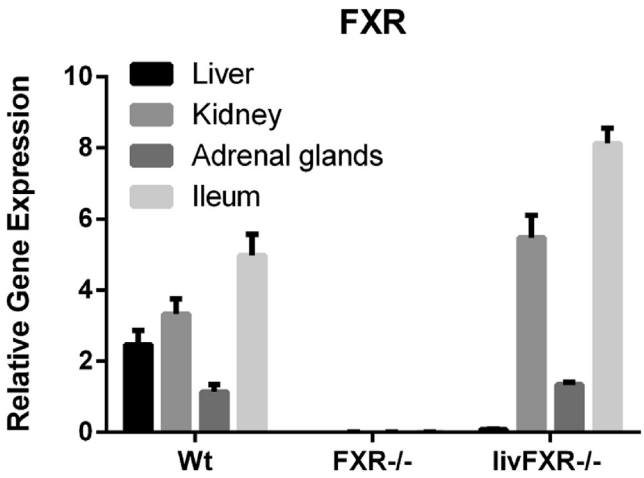

Supplementary Figure 1. Validation of FXR depletion in $FXR^{-/-}$ and liver $FXR^{-/-}$ mice. Determination of FXR expression in liver and kidney tissue of Wt, $FXR^{-/-}$, and liver $FXR^{-/-}$ mice by RT-qPCR. Disruption of FXR was validated, using primers Fw: 5′-acagctaatgaggacgacag -3′, Rv: 5′-gatttcctgaggcattctctg-3′ and expression was normalized to cyclophilin. (5′-ggagatggcacaggaggaa-3′, Rv: 5′-gcccgtagtgcttcagctt-3′). Expression is relative to cyclophilin. Data are represented as mean ± SEM.

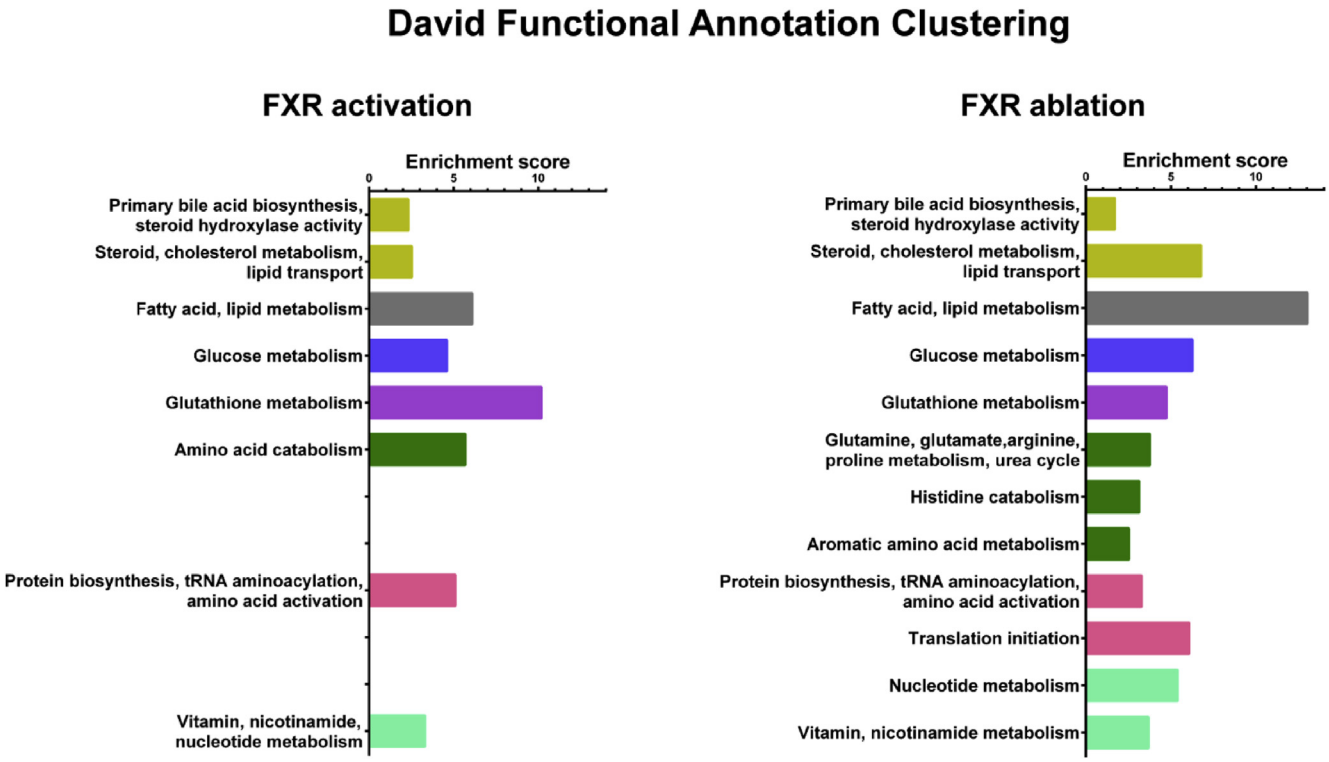

Supplementary Figure 2. Liver proteomic analysis reveals regulation of nutrient metabolism by FXR activation/ablation. David Gene Ontology cluster analysis of metabolic processes enriched upon FXR activation/ablation. Differential protein changes were included in the analysis when $\geq$1.3-fold.

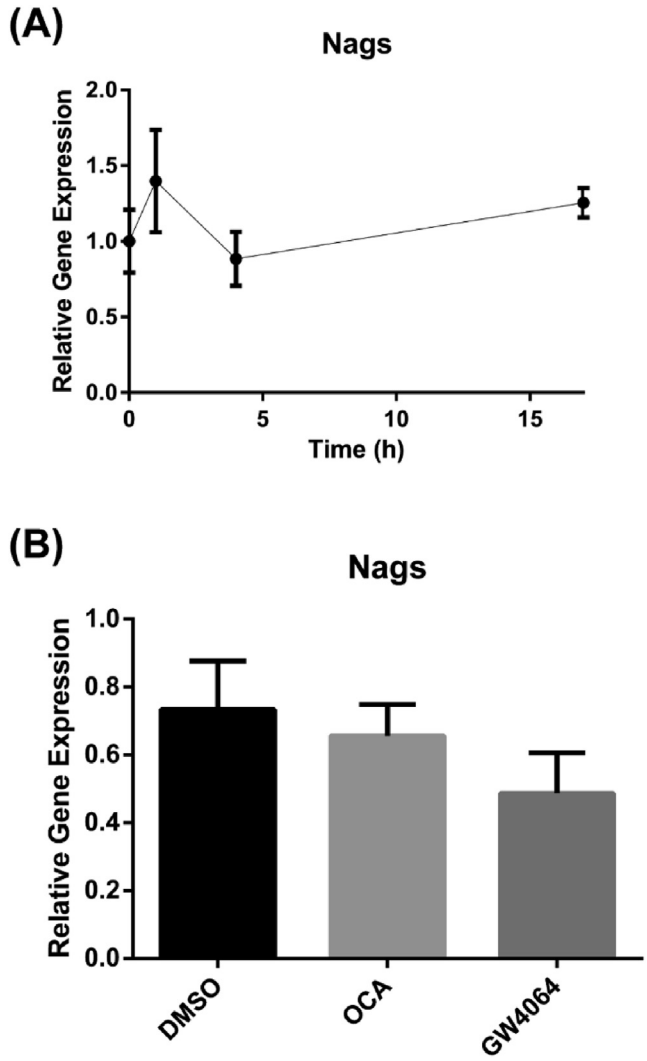

Supplementary Figure 3. *Nags* expression does not change upon FXR activation. (*A*, *B*) Relative gene expression of *Nags* was investigated by qRT-PCR in primary hepatocytes incubated with DMSO or 1 μM OCA for 0, 1, 4, or 17 hours (*A*) and with DMSO or OCA or GW4064 for 6 hours and in the last hour before harvesting with 2 mM NH_4Cl, 0.4 mM glutamine, 0.6 mM ornithine, 10 mM HEPES in Hank's balanced salt solution (mean $\pm$ SD, n=3, no significant changes).

Supplementary Table 1. Regulatory Sites Determined by Chromatin Immunoprecipitation Quantitative Polymerase Chain Reaction for Farnesoid X Receptor in Liver Extracts

Gene	No. of peaks analyzed	Genomic location of the peak (Chr:start−end)	Peak distance from TSS, *bp*	IR-1 motif in the peak (AGGTCANTGACCTN)	ChIP-qPCR primers (5′→3′)
Cps1	1	chr1:67124225−67124829	−45,073	AGAGCCAATGACCC	FW gttgtttcagattagcaatgttgac RV cacatttgatttgcacagtgg
	2	chr1:67125141−67125712	−44,174	AAGGCCATTGACTC	FW atgttcaactcaaagatggctct RV aggcctttggaacaaataagg
	3	chr1:67190203−67191017	+21010	GGGTCAATGGCTGC	FW ggctggctaccaagagtctg RV cctatctgacttctcacctttttcc
Glul	1	chr1:155746632−155747475	−5	CGGCCAATGGCCTC	FW cacagttcctcggccaat RV ggtacttttattgacagcttgtgc
Ass1	1	chr2:31315817−31316207	−9777	AGGGCAGAGACCGC	FW gggctctaccgcttgactg RV gcaggatgtagacgctctgg
Asl	1	chr5:130497223−130499011	−2084	GGGTCCTTGACCTC	FW tgagttacgacggcctgat RV aaagtccagcccttgttcct
Hal	1	chr10:92950852−92952224	−99	GGGTCAGAGAACTA	FW agtgggctcagctacccata RV gtgttcctttggcctttctg
Prodh	1	chr16:18083266−18084303	+5499	AGGCCACTGGCCCT	FW ggctcctccccaggtaacta RV agtggcctcacatgactgc

Supplementary Table 2. Quantitative Reverse Transcription Polymerase Chain Reaction Primers

Gene	Sequence (5′→3′)
Rat	
36B4	FW cgggaaggctgtggtgctgatg
	RV tcggtgaggtcctccttggtgaac
Shp	FW ggagtctttctggagccttg
	RV cacatctgggttgaagagga
Cyp7a1	FW atctcaagcaaacaccattcc
	RV ttgatgatgctgtctagtacc
Glul	FW tcaagtataaccggaagcccg
	RV gaaagggtggccgtctgtt
Cps1	FW atgctctgggtgggttagg
	RV aggatctggttggtcatagca
Ass1	FW ggagaaccgcttcattgg
	RV tgagcgtggtaaaggatggt
Asl	FW aagccatccgaagctgtttg
	RV cttgtccccgcctcctgt
Hal	FW tgaaggcgatgtaatgtctcc
	RV cccatccaaggcaatgtact
Prodh	FW gagcgcaaagaaatggagtc
	RV gggtggacctgatactgcttc
Nags	FW cagattcggctcatcgtgga
	RV tgccacagcccttgttactg
Mouse	
Cyclophilin	FW ggagatggcacaggaggaa
	RV gcccgtagtgcttcagctt
Bsep	FW aagctacatctgccttagacacagaa
	RV caatacaggtccgaccctctct
Glul	FW ccgcctcgctctcctgacc
	RV cgggtcttgcagcgcagtc
Gls2	FW ccgtggtgaacctgctattt
	RV tgcgggaatcatagtccttc
Ass1	FW acacctcctgcatcctcgt
	RV gctcacatcctcaatgaacacct
Nags	FW cttcggagagacctgcaaac
	RV ccgaaccagaagaagatcca
Prodh	FW gcaccacgagcagttgttc
	RV ctttgttgtgccggatcagag
FXR	FW acagctaatgaggacgacag
	RV gatttcctgaggcattctctg

Supplementary Table 3. Farnesoid X Receptor$^{-/-}$/Wild-Type Fold-Change in Liver Expression of Bile Acid Metabolism-Related Proteins

Protein	Fold-change Wt OCA/Wt Veh	Fold-change FXR$^{-/-}$ Veh/Wt Veh
BA synthesis		
Cyp8b1	−7.91	2.42
Cyp7a1	ND	5.04
Cyp7b1	−2.96	−14.88
Hsd3b7	−1.43	−2.00
Cyp27a1	−1.11	−2.35
Ces1f	−1.98	−1.12
Cyp39a1	−1.13	−2.46
BA conjugation/taurine synthesis		
Baat	−1.21	1.87
Csad	−1.55	9.29
BA/phosphatidylcholine transport		
Abcb11/Bsep	2.15	−5.31
Abcb4/Mdr3	1.68	1.39
Abcc2/Mrp2	1.50	−1.19
Pcyt1a	2.36	−1.62
Slc10a1/Ntcp	1.04	−4.12
Slco1a1/Oatp1	−1.49	−3.13
Abcc3/Mrp3	1.95	16.19

Supplementary Table 4. Farnesoid X Receptor$^{-/-}$/Wild-Type Fold-Change in Liver Expression of Amino Acid Metabolism-Related Proteins

Protein	Fold-change Wt OCA/Wt Veh	Fold-change FXR$^{-/-}$ Veh/Wt Veh
Histidine degradation		
Hal	2.33	−2.16
Uroc1	1.83	−1.58
Amdhd1	1.86	−2.93
Ftcd	2.26	−1.75
Proline degradation		
Prodh	1.49	−2.30
Tryptophan degradation		
Tdo2	2.56	−2.25
Kynu	1.47	−1.36
Methionine degradation		
Mat1a	1.56	1.07
Ahcy	1.50	−2.02
Cth	2.16	−1.04
Phenylalanine degradation		
Pah	1.47	−1.23
Lysine degradation		
Agphd1	1.48	−1.78
Urea cycle		
Ass1	2.31	−1.74
Asl	1.36	−1.53
Arg1	1.36	−1.53
Cps1	−1.24	−2.05
Nags	−1.39	−3.67
Urea cycle−related		
Oat	2.43	3.01
Got1	1.30	−2.14
Gls2	1.12	−5.82
Glud1	−1.43	−1.50
Glutamine synthesis		
Glul	1.52	−2.22

Supplementary Table 5. Farnesoid X Receptor$^{-/-}$/Wild-Type Fold-Change in Concentration of Amino Acids in Liver Extracts

Amino acid	Fold-change FXR$^{-/-}$ Veh/Wt Veh	*P* value	Fold-change FXR$^{-/-}$ OCA/Wt Veh	*P* value
Glu	3.30	.005**	3.78	.000**
Pip	1.78	.085	2.01	.045
Gln	1.62	.003**	1.68	.002**
Asp	1.58	.051	1.68	.025*
His	1.39	.001**	1.29	.005**
Pro	1.05	.694	−1.03	.770
Arg	1.05	.292	1.05	.453
Ser	1.00	.993	−1.18	.370
Trp	−1.01	.933	−1.15	.211
Thr	−1.07	.615	−1.26	.069
Ile	−1.13	.466	−1.13	.398
Val	−1.14	.455	−1.28	.135
Phe	−1.14	.286	−1.34	.011*
Lys	−1.14	.255	−1.22	.047
Ala	−1.20	.109	−1.27	.023*
Orn	−1.20	.243	−1.54	.007**
Leu	−1.21	.270	−1.46	.018*
Tyr	−1.21	.162	−1.41	.015*
Gly	−1.23	.154	−1.54	.000**
Met	−1.33	.115	−1.70	.001**
Asn	−1.38	.112	−1.41	.074
OH-Pro	−1.63	.006**	−1.59	.006**
Cit	−2.76	.079	−8.93	.005**

Supplementary Table 6. Obeticholic Acid/Dimethyl Sulfoxide Fold-Change Concentration of Amino Acids in Medium of Primary Hepatocytes

Amino acid	Fold-change	*P* value
Glutamic acid	−1.65	.003**
Alanine	−1.63	.001**
Isoleucine	−1.62	.010*
Leucine	−1.60	.006**
Phenylalanine	−1.58	.012*
Valine	−1.58	.002**
Tyrosine	−1.56	.055
Arginine	−1.55	.100
Proline	−1.49	.009*
Histidine	−1.43	.018*
Methionine	−1.43	.019*
Threonine	−1.40	.043*
Lysine	−1.38	.038*
Serine	−1.29	.016*
Aspartic acid	−1.26	.243
Tryptophan	−1.19	.038*
Glutamine	−1.16	.027*
Ornithine	1.00	.809

NOTE. Determination of amino acid concentrations in medium of primary hepatocytes treated for 16 hours with OCA or DMSO and in the last hour before harvesting with 2 mM NH_4Cl, 0.4 mM glutamine and 0.6 mM ornithine. OCA/DMSO fold-change in concentrations of amino acids and related significance are shown.